Analysis of the dynamic performance of a MEA-based carbon capture unit for coal-fired power plants

A.M. van de Haar

Master of Science Thesis

TU Delft Delft University of Technology

Report: P&E-2533

Process & Energy Delft

Analysis of the dynamic performance of a MEA-based carbon capture unit for coal-fired power plants

Master of Science Thesis

For the degree of Master of Science in Mechanical Engineering at Delft University of Technology

A.M. van de Haar

June 12, 2013

Faculty of Mechanical, Maritime and Materials Engineering · Delft University of Technology

The picture of the E.ON Maasvlakte power plant on the front cover is taken by Chris10 and published on Panoramio (http://www.panoramio.com/). Usage of the picture has been approved by E.ON Benelux. E.ON Benelux and Chris10 are hereby gratefully acknowledged.

Delft University of Technology
Department of Process and Energy
Faculty Mechanical, Maritime and Materials Engineering (3Me)

The undersigned hereby certify that they have read and recommend to the Faculty of Mechanical, Maritime and Materials Engineering for acceptance a thesis entitled

Analysis of the dynamic performance of a MEA-based carbon capture unit for coal-fired power plants

by

A.M. van de Haar

in partial fulfillment of the requirements for the degree of

Master of Science Mechanical Engineering

Dated: June 12, 2013

Supervisors:

Prof.dr. P. Colonna	Dipl.-Ing. C. Trapp
Ir. R.C.F. de Kler	

Exam committee:

Prof.dr. P. Colonna	Prof.dr.ir. B.J. Boersma
Dipl.-Ing. C. Trapp	Ir. R.C.F. de Kler
Dr.ir. X.J.A. Bombois	Prof.Dr.-Ing. G. Schmitz

Abstract

In order to limit global average temperature rise, the greenhouse gas (GHG) emissions should be reduced significantly. A large part of this emissions is caused by the energy-related industry. Although the share of renewable energy sources (RES) is increasing rapidly, the dependency on fossil fuels, as for example coal, is likely to remain high in the following decades. One of the possibilities to reduce our carbon footprint is carbon capture and storage (CCS) technology, whereby carbon dioxide (CO_2) is captured and kept for long-term storage in empty gas or oil fields. CCS is a vital component of the low-carbon technologies portfolio which will hopefully meet the CO_2 emission reduction targets. Growth of RES like wind and solar will demand more flexibly operating power plants.

There are different options for CCS, namely pre-combustion capture, post-combustion capture and oxyfuel combustion. Post-combustion capture (PCC) has significant advantages over other capture technologies as it can not only be applied to greenfield power plants but also to existing power plants in a retrofit application. To minimize the efficiency-penalty on the power plant, integration of the capture plant with the power plant is required. Integration of the power plant and capture unit could impose constraints on the power plant in transient operation. Currently, there is no operational experience with PCC technology at full or demonstration scale. Modeling of the integrated system is therefore essential to investigate its performance and controllability during transient operation.

In this study the constraints and flexibility during transient operation of a PCC unit are assessed using an equilibrium-based dynamic model of the capture unit. The dynamic models are developed in Modelica, an open-source, object-oriented and equation-based language for the modeling of physical systems. Where possible, existing model libraries are used or modified in order to obtain a complete model of the capture unit. The plant utilizes monoethanolamine (MEA) as the absorption fluid. The dynamic model is validated with open-loop step response tests performed at the TNO pilot plant.

Based on the performed validation, it can be concluded that the transient responses in terms of trend and time constant of the capture rate, absorber temperatures and solvent CO_2 loading are in good agreement with the experiments. Although accurate steady-state predictions are not of main interest for the dynamic validation, mismatches are observed in steady-state predictions of absorber temperatures and solvent CO_2 loading. In order to assess the operational flexibility of a capture unit, three test cases were defined and simulated with the validated capture unit model. These test cases are based on a normal load variation of a coal-fired power plant. From the case results it can be observed that the required stabilization time of the capture plant is closely related to the total liquid residence time. In general, it can be concluded that the capture plant has a smooth response to load fluctuations of the power plant, which is desirable regarding the integration with the power plant.

Table of Contents

List of Figures

List of Tables

Acknowledgements

Firstly, I would like to thank my supervisor Piero Colonna for his guidance and time devoted to this project. His structured approach to dynamic modeling formed the basis of this research. His supervision motivated me to achieve great results and to write a thesis of high quality. My sincere thanks also go to Carsten Trapp, who has been always available to help me during this research.

My thanks go also to my supervisor at TNO, Robert de Kler. His practical approach and experiences were very useful. Hereby I also would like to thank the other colleagues at TNO who helped me with doing experiments at the pilot plant and the analysis of the solvent in the lab.

I would like to thank Kai Wellner and Gerhard Schmitz from TU Hamburg-Harburg for making available their model library. The meetings we had were in my opinion very helpful for both them and me as they were very interested in the validation and implementation of their models. This interest really motivated me to finish the research.

Finally, I want to thank my family and friends for their support and patience during my study and particularly this project.

Delft, University of Technology A.M. van de Haar
June 12, 2013

Chapter 1

Introduction

1-1 Background information

1-1-1 Carbon capture and storage

Climate change and global warming is very likely to be caused by increased concentrations of greenhouse gases (GHG) produced by human activities. An important greenhouse gas is carbon dioxide (CO_2) and burning carbon-based fuels has increased its atmospheric concentrations rapidly since the industrial revolution. A large share of this increase in CO_2 emissions is caused by the fossil fuel-based power industry. In 2010, electricity and heat generation accounted for 41% of the world's CO_2 emissions [1]. One of the options to mitigate CO_2 emissions is by applying carbon capture and storage (CCS). CCS is a process consisting of the separation of CO_2 from industrial and energy-related sources, transport to a storage location and long-term isolation from the atmosphere[2]. The International Energy Agency (IEA) estimated that 17% of the required reduction could be achieved with CCS(see Figure 1-1) and therefore CCS is a vital component of the low-carbon technologies to meet the CO_2 emission reduction. In addition, the IEA estimated that without CCS, the overall costs to reduce the emissions by 50% over the period to 2050 would increase by 70%[3].

CO_2 capture can be applied to different fossil-fuel power plants and therefore one distinguishes between different capture technologies (Figure 1-2):

- Post-combustion
- Pre-combustion
- Oxyfuel combustion

Post-combustion capture is a technology in which CO_2 is captured from flue gas of a conventional combustion power plant. Pre-combustion capture is the capture of CO_2 from synthesis gas before it is burned. This eases the capture of CO_2, as the CO_2 concentration is significantly higher than in flue gas for a post-combustion capture application. In the energy industry pre-combustion capture is applied in an Integrated Gasification Combined Cycle (IGCC). The main disadvantage is that it can only be applied to greenfield power plants as large modifications to the fuel processing are required. In an oxyfuel combustion process the fuel

is combusted with oxygen instead of air. The flue gas contains mainly CO_2, which makes it easier to capture CO_2 from it. Although oxyfuel-combustion power plant have a higher efficiency, combustion with pure oxygen leads to high flue gas temperatures which requires special materials.
The pre-combustion capture technology is considered to be the most mature technology as it is the only technology which is currently commercially deployed on full-scale for power plants (Kemper County IGCC 582MWe) and in general of the three technology options the most chosen technology in planned project worldwide[4]. For post-combustion capture the only project in the execution phase is at a demonstration scale (Boundary Dam Integrated CCS Demonstration Project)[4]. Carbon capture is in the natural gas and chemical processing industry already a mature technology. The main reason for that is that in power plants generally the CO_2 concentration is lower, which makes CO_2 capture more difficult.

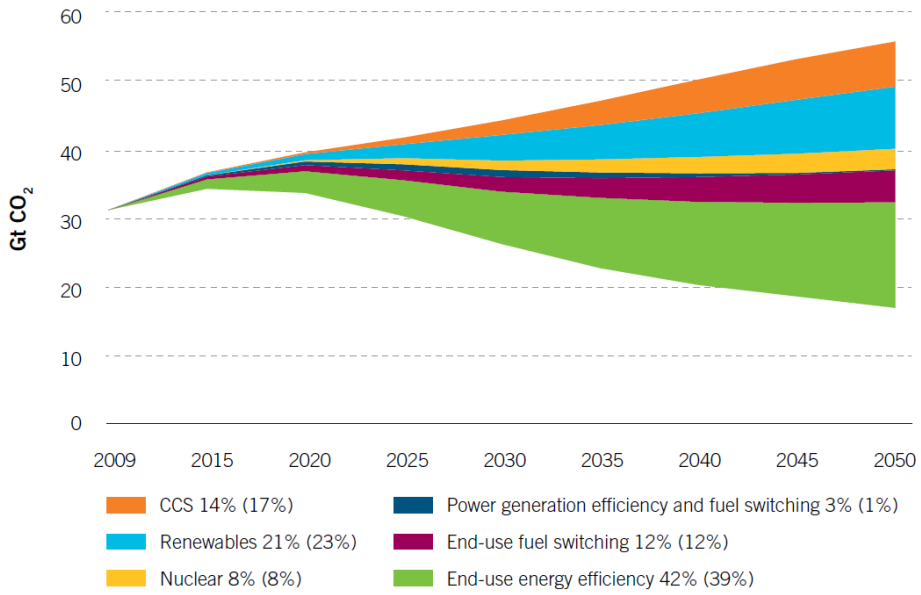

Figure 1-1: Energy-related CO_2 emissions by technology [5][1]

1-1-2 Post-combustion capture

Technology options

Post-combustion capture (PCC) has a significant advantage over other technologies. The application of this capture technology does not require substantial modifications in power plants and can therefore be easily implemented as retrofit to existing conventional coal-fired plants. Large investments for the development of new power plants are not necessary. Currently, three main PCC processes are applied: absorption, adsorption and membrane separation. In the absorption process, CO_2 is removed by dissolving it into a liquid solution in an absorber. In a stripper the solvent is regenerated and CO_2 is released by increasing the temperature. In adsorption, CO_2 is adsorbed on a solid surface. The regeneration of the adsorbent can be achieved by pressure decrease or temperature increase. In membrane separation the CO_2 is

[1]Percentages represent share of cumulative emission reductions to 2050. Percentages in brackets represent share of emission reductions in the year 2050.

removed by use of a membrane which selectively permeates CO_2. An advantage compared to absorption is that the required regeneration energy for adsorption and membrane separation is significantly lower. The latter two technologies are still in an earlier stage of development and therefore are currently only applied on a few kilowatt scale. Hence, at present the absorption process is the most applied technology for post-combustion CO_2 capture. Large quantities of heat and other auxiliary power are required for CO_2 capture and compression. The main challenge is to reduce the high efficiency reduction of the application PCC on power plants.

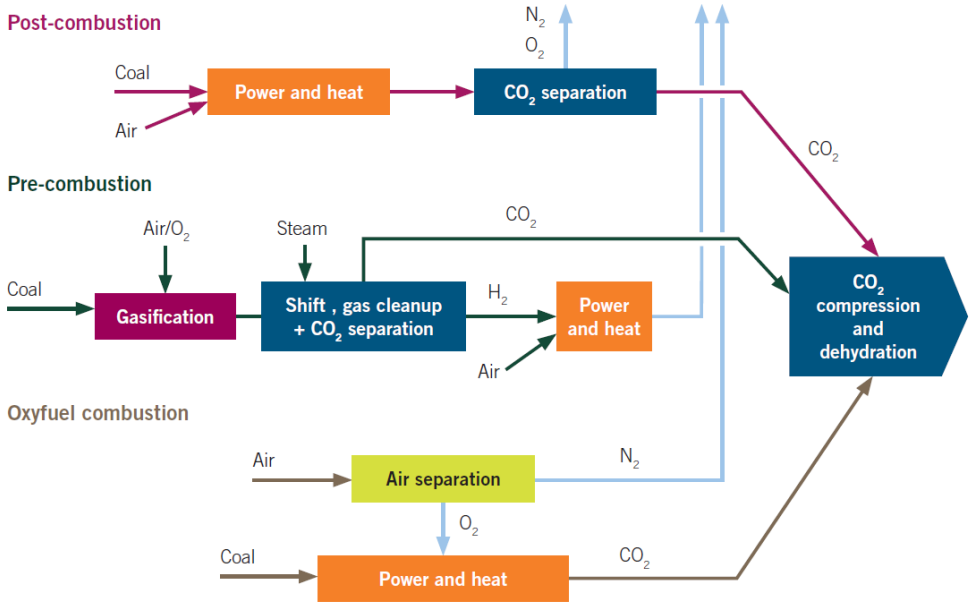

Figure 1-2: Overview of the different technology options for CO_2 capture [6]

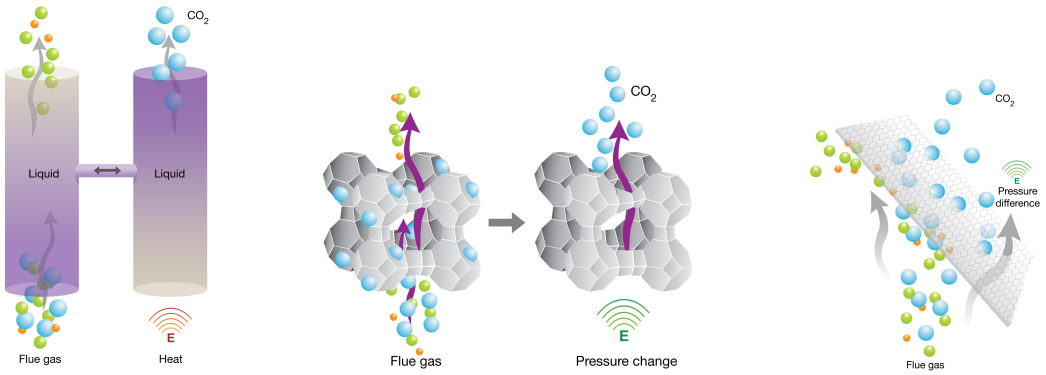

Figure 1-3: Different process options for post-combustion CO_2 capture [7]

Chemical absorption

Currently, chemical absorption is in comparison to physical absorption and membrane separation the preferred technology option for Post-combustion capture (PCC) as it is a feasible, low cost solution to capture CO_2 from flue gas at low CO_2 partial pressure. In chemical absorption, the CO_2 is absorbed and reacts with the solvent(see Fig.1-4). In the stripper and reboiler the CO_2 rich solvent is regenerated with heat and returned as CO_2 lean solvent to the absorber. Suitable solvent for chemical absorption are amine-based solvents, ammonia and carbonates. Monoethanolamine(MEA) is an amine-based solvent which is currently considered as a baseline solvent for its high reaction rate with CO_2 and low solvent cost. However, the regeneration heat required to release the CO_2 is relatively high. The regeneration heat demand decreases for increasing solvent concentration. However, monoethanolamine (MEA) degrades at temperature levels above 120 °C and in the presence of SO_x, NO_x or oxygen in the flue gas. The degradation products are highly corrosive and cause further degradation of solvent. The risk for corrosion increases with higher amine concentration, therefore MEA-based solvents are commercially applied up to a concentration of 30 weight percent. To minimize the efficiency penalty the heat demand for the reboiler is provided by extracting steam from the power plant steam cycle. However, this integration also affects the power plant dynamics and its ability to ramp the electricity production up or down. A study of the integrated system is necessary to understand the performance of such a combined system under transient operation.

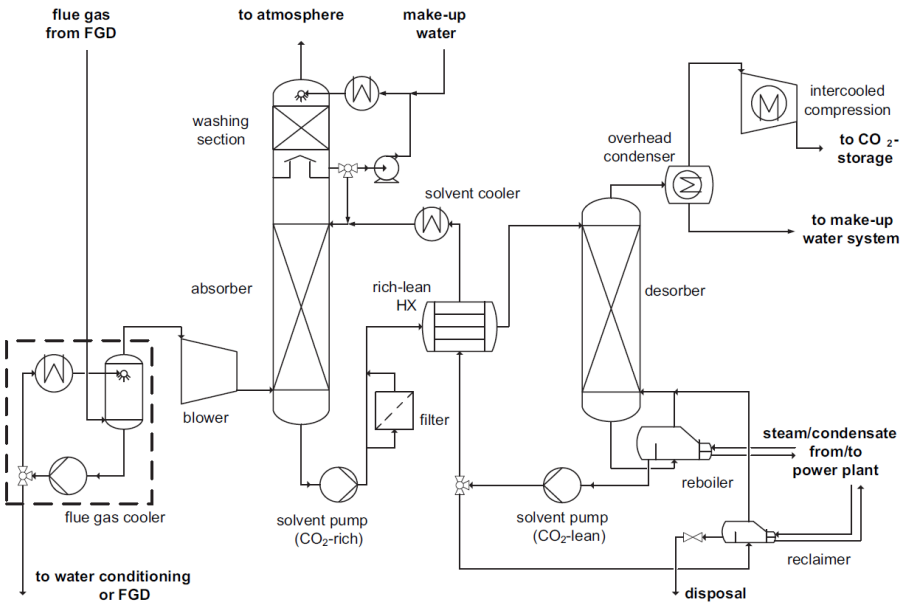

Figure 1-4: A typical PFD for a chemical absorption based CO_2 capture plant [8]

1-1-3 Dynamic modeling

Dynamic modeling of energy processes

There are different approaches for the dynamic modeling of energy processes. Both distributed and lumped parameter models are suitable for dynamic process modeling depending on the purpose. In case of system modeling, the lumped parameters approach is the most suitable since it is less complex and leads therefore to shorter simulation time with capturing the relevant dynamic performance of the process. The development of a dynamic model leads to a set of differential and algebraic equations (DAEs), i.e.,

$$F(t, y, \dot{y}) = 0 \tag{1-1}$$

Transforming this equations into a system of ordinary differential equations (ODEs) in the form of

$$\dot{y} = G(t, y) \tag{1-2}$$

makes the equations easier to solve. This can be achieved by differentiation of the algebraic equations. A disadvantage of this method is that after this mathematical manipulations the link of the equations with physical representation is lost. The (differential) index of the system is defined as the minimum number of differentiations with respect to time to convert the system to a set of ODEs. Dynamic process models can be divided into low index models (index 0 and 1) and high index models (index two and higher) [9]. With increasing index the difficulty to solve these equations increase. For additional information on the index problem and solving a set of DAEs one might consult References [10]-[13].

A distinction can be made between the simultaneous and modular approach. In the modular approach the model is decomposed into modules in which the output of every module is computed as a function of input or internal variables. In the simultaneous approach the system is modeled as a whole, meaning that all model equations are implemented in a single routine. It has the advantage of being the most computational efficient. However, it is hard to modify a simultaneous model for a different process configuration. Therefore a modular approach would be more preferable since it enables the user to increase the level of complexity where necessary and to re-use existing model components.

To develop these modular models two approaches can be followed: the causal (procedural) of a-causal (declarative) approach. In the causal approach, systems are decomposed into computational block diagram structures with predefined causal interactions. The input variables for the system should be decided a priori which limits the user to a certain choice of boundary and initial conditions. The bilateral coupling principle can be used to choose input and output variables of the system and its modules to assure causal modeling. If there is a power transfer across the system boundary then it is possible to define a generic potential variable $p(t)$ and a generic flow variable $f(t)$. The product of these variables is a measure of the power transfer between the component and its surroundings. Variables that are bilaterally coupled should not be both imposed as inputs at the same boundary interface. Examples of bilaterally coupled variables are listed in Table 1-1.

Modules can be characterized either as a storage or a resistive module. A module in which one of the conserved variables (mass, momentum or energy) is accumulated is called a storage module. A storage module is characterized by dynamic conservation laws in the form of

$$S\frac{\mathrm{d}p(t)}{\mathrm{d}t} = f(t) \tag{1-3}$$

The input variable for a storage module is the flow and the output variable is the potential. A resistive module is a module in which accumulation of conserved variables is neglected, which results into an algebraic equation in the form of

$$f(t) = R \cdot p(t) \tag{1-4}$$

The input variable for a resistive module is the potential and the output variable is the flow. To keep causality, storage and resistive modules should be connected in series (see Fig. 1-5). In this study, causality is kept by use of this bilateral coupling principle. The interested reader might consult References [14]-[17] for additional information on dynamic process modeling paradigms.

Table 1-1: Examples of bilaterally coupled potential and flow variables [18]

Potential variable	Flow variable	Type of power transfer
Pressure	Mass flow	Mechanical
Temperature	Heat flux	Thermal
Rotational speed	Torque	Mechanical
Velocity	Force	Mechanical
Voltage	Current	Electrical

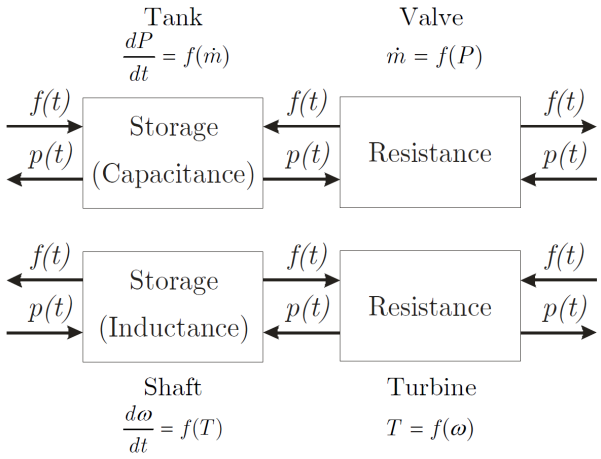

Figure 1-5: Examples of the bilateral coupling principle [19]

Dynamic modeling of post-combustion capture units

There are few studies on dynamic modeling of post-combustion capture units. Kvamsdal et al.[20] developed a dynamic model for the absorber only. The model is validated against data of a capture pilot plant. With the absorber model, a start-up and part-load procedure is simulated. It was concluded that the dynamic model is representing the dynamic behaviour of the column, although only validation against steady-state data was performed. An integrated model including a dynamic model of the stripper is needed to evaluate operational challenges regarding a stable and optimized control. Dietl et al.[21] developed a dynamic model of the whole cycle of a capture unit using the Modelica library ThermalSeparation[22]. The solvent used in the capture unit is an amino-acid salt. Different control strategies to handle a temporary reduction in steam mass flow are investigated using the model. It was concluded that the

time to reach steady state was the highest if the solvent flow rate is not reduced for a reduction in steam flow rate. In addition, the dynamic performance of the entire capture unit model is compared with single models of the absorber and stripper. Comparison shows that during the first minutes the response is similar, but on longer time scale the results are different. This is due to the fact that interaction between absorber and stripper is not accounted for as the models are not connected. Lawal et al.[23] developed a model of a MEA-based capture plant integrated with a dynamic model of a 500MWe power plant. The power plant model was validated against steady-state data from a coal-fired power plant. After dynamic analysis, it is concluded that the carbon capture unit (CCU) has a slower response than the power plant.

None of the previously mentioned studies included dynamic validation of the dynamic model in the analysis, mainly due to the lack of experimental data for transient operation. Akesson et al.[24] developed a model of the capture unit and validated it with open-loop tests performed at a pilot capture plant [25]. During these tests the reboiler duty, the flue gas flow and the solvent flow were disturbed. The model showed similar responses to the disturbances in comparison with the experiments. To use the model for dynamic optimization it is reduced by replacing the chemical reactions in the liquid phase by equilibrium data. For the dynamic optimization only a model of the stripper column and the reboiler is used. In order to obtain more reliable results, a validated model is required to study the dynamic performance of the complete system and to test possible control strategies.

1-2 Objectives

The objectives of this study are to investigate operational constraints and flexibility during transient performance of a post-combustion carbon capture unit for a coal-fired power plant. Constraints and flexibility concern the interaction of the CCU with the power plant which are integrated via the flue gas flow and the reboiler steam flow. Only load variation (ramping up and down) will be considered as start-up and shut-down procedures have other relevant phenomena compared to the ones for load variation. The following objectives are formulated:

1. Development of a detailed dynamic model of a post-combustion capture unit
2. Design and execution of transient experiments for model validation purposes
3. Validation of the dynamic capture unit model against experimental data
4. Implementation of a control structure allowing for load variation
5. Analysis of transient performance of CCU with focus on operational constraints and flexibility

1-3 Approach

The analysis of the transient operation of the capture unit is performed by means of dynamic process modeling and simulation. A dynamic model has been developed based on the process configuration and geometry of the TNO pilot capture plant at the site of the Maasvlakte power plant in Rotterdam. This pilot is designed to process up to 1500 Nm^3/h of flue gas and is operated with MEA as the absorption fluid. An available steady-state model is adapted to provide initial values for the dynamic model.

For the development of the dynamic model the open-source Modelica language [26] has been used. The Modelica language is fully a-causal and equation-based and therefore supports a object-oriented approach to dynamic modeling of physical systems. The modular approach has been applied to facilitate model adaptations and the re-use of developed model components. The bilateral coupling principle has been applied to keep the index of the system at one.

The modular approach also enables the user to re-use model components of existing libraries. For the modeling of the CCU unit the ThermalSeparation library[22] developed by Hamburg University of Technology has been used. The library makes available models for the absorber, stripper and reboiler as well as media libraries. These modules are re-used where possible and partly modified if necessary. Models of heat transfer and rotating equipment of the ThermoPower library [27] are adapted and implemented to develop a complete dynamic model of the capture unit. ThermoPower is an open Modelica library for the modeling of thermal power plants and energy conversion systems developed by Politecnico di Milano and Delft University of Technology. The library contains thermo-hydraulic modules to model components, such as heat exhangers, valves and pumps. A commercial software tool [28] has been used as the modeling environment. This software tool makes available a user interface and executes symbolic manipulations to solve the set of equations defined by the Modelica model.

The dynamic model is validated against experimental data obtained from open-loop step response tests which were performed at the pilot capture plant in November 2012. With open-loop tests the influence of involved process controllers can be eliminated in order to observe the process response. Based on the analysis of the experimental tests a control concept is defined for the case whereby the capture unit is integrated with a coal-fired power plant. The defined control concept is implemented in the validated capture unit model and subsequently transient simulations are performed.

1-4 Thesis outline

Chapter 2 presents detailed information on the pilot capture plant. The configuration, operating conditions and the control structure of the pilot plant are described.

Chapter 3 describes the development of the dynamic capture unit model. First, an existing steady-state model is improved and modified. Then, the development of the dynamic model is described.

Chapter 4 presents the validation of the dynamic model with pilot plant experiments. A test plan has been defined, and the validation results are presented and discussed.

Chapter 5 describes the dynamic analysis of the dynamic capture unit model. Proposed test cases are described and explained. The results of proposed test cases are shown and discussed.

Finally, the conclusions and recommendations are drawn in Chapter 6.

Chapter 2

Capture pilot plant

As a part of the CATO-2[29] research program, TNO has commissioned a post-combustion capture pilot plant at the Maasvlakte power plant in Rotterdam, the Netherlands in 2008. The capture plant can process up to 1500 Nm^3/h flue gas and capture 250 kg/h carbon dioxide (CO_2). The flue gas flow is equivalent to 0.3 MWe power output of a coal-fired power plant. An overview of the capture pilot plant is given in Figure 2-1.

2-1 Configuration

The design of the capture pilot plant is based on a standard amine-based CO_2 capture process. This section describes the working principle of the different process units. The processed flue gas is a slipstream taken downstream the flue gas desulphurization (FGD) unit of the power plant. The pilot plant consist of the following consecutive process units:

- knock out drum
- caustic scrubber
- blower
- absorber tower with washing section
- lean-rich heat exchanger
- stripping tower with reboiler
- condenser

A simplified Process Flow Diagram (PFD) of the capture pilot plant is given in Figure 2-2.

2-1-1 Flue gas conditioning

A slip stream of the flue gas exiting the FGD unit of the power plant enters the capture plant in a knock-out drum to knock-out condensate water in the flue gas. Then the flue gas is scrubbed and cooled in the caustic scrubber. Flue gas exiting the FGD unit of the power plant still contains sulphur dioxide (SO_2). SO_2 forms heat stable salts with the solvent and therefore its concentration must be reduced. The caustic scrubber reduces the SO_2 content to about 1.0 ppm. The caustic scrubber contains a recirculation system to cool the flue gas.

Figure 2-1: The TNO pilot capture plant at the EOn site at the Maasvlakte (Rotterdam, the Netherlands)

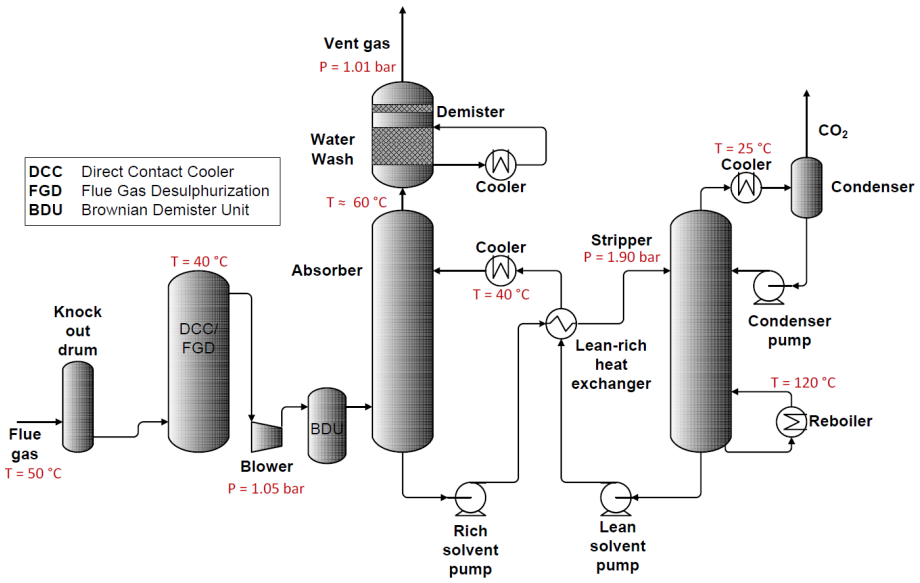

Figure 2-2: A simplified PFD of the capture pilot plant at the Maasvlakte, Rotterdam

Caustic soda is used to regulate the pH value in the scrub solution within a narrow band. The pressure of the flue gas entering the caustic scrubber is high enough to overcome the pressure drop of the scrubber. Therefore, the blower to overcome the pressure drop in the absorber column is placed after the scrubber. Downstream the blower the flue gas is led trough the Brownian Demister Unit (BDU). The BDU is a filter to remove very fine mist particles of less than 2 microns. This is necessary to minimize solvent emission due to aerosols which form fine particles.

2-1-2 Absorber tower

Leaving the BDU the flue gas enters the absorber. In the absorber tower flue gas passes through four packed beds designed for sufficient contact time for CO_2 absorption. The inlet position of the lean solvent entering the absorber column can be varied depending on the

desired CO_2 capture-rate. This inlet position can be chosen on top of each of the four packed beds. Between the packed beds liquid distributors are installed to redistribute the solvent over the packing. In the absorber sump the liquid exiting the absorber bed is collected. The sump is designed such that it can store approximately 60% of the solvent during shut-down. As the absorption process is an exothermic reaction, the cleaned (sweet) gas has a higher temperature than the inlet flue gas. The clean vent gas exiting the absorber top passes through a water wash section mounted on top of the absorber. In this section water and solvent present in the gas are condensed and returned to the absorber. With the water wash the water balance in the system is controlled and solvent loss is reduced. Additionally a demister section on top of the absorber reduces the loss of solvent by removing small particles.

2-1-3 Stripper tower

Before the rich solution enters the stripper it is pumped through the lean-rich heat exchanger where it is preheated by the hot lean solution leaving the stripper. Preheating reduces the reboiler duty and enhances stripping in the top section of the stripper tower. The stripper tower consist of two sections of packed beds in which CO_2 is stripped from the rich solution. The solution exiting the stripper enters the reboiler where it is partially evaporated. The resulting vapour is recyled to the stripper tower. The hot lean solution is accumulated in the stripper sump and then pumped through the lean-rich heat exchanger. Before entering the absorber, the solution is cooled by the lean solvent cooler. The CO_2 product flow leaving the stripper top is cooled in a condenser and condenser condensate is collected in a condensate tank and recycled to the stripper tower. Both product streams, the clean gas exiting the absorber as the CO_2 leaving the stripper top are vented back into the power plant chimney, as the CO_2 compression and storage system is not included in the pilot plant.

Table 2-1: Normal operating conditions of the capture pilot plant at the Maasvlakte, Rotterdam

Variable	Value	Unit
Flue gas flow	800	m^3/h
Solvent flow	3.2	ton/h
Stripper pressure	1.9	bara
Lean solution temperature	40	°C
CO_2 product temperature	25	°C
Flue gas absorber inlet temperature	40	°C
MEA concentration	30	wt.%
CO_2 capture rate	90	%

2-2 Operating conditions and control structure

A simplified process and instrumentation diagram (P&ID) of the pilot capture plant is given in Figure 2-3. The flue gas flow is controlled by a valve downstream of the knock-out drum. The additional pressure drop caused by the later installed BDU and the limited capacity of the blower decreases the maximum possible flue gas flow to 800 Nm^3/h. With a solvent flow of 3.2 ton/h, this results in a capture rate of approximately 90%. The solvent mass flow is controlled by the valve downstream the solvent cooler. The minimum solvent mass flow rate is 3 ton/h, below that value stable flow control is not possible. The pressure in the stripper

is controlled by a valve at the outlet of the stripper with a nominal set point for the absolute pressure of 1.9 bar. The temperature of the reboiler is controlled by regulating the steam flow generated by an electric-powered steam generator. The reboiler temperature controller has a nominal set point of 120 °C, as for lower temperatures the capture rate decreases and at higher temperatures degradation of solvent will take place. Therefore, the reboiler temperature is always controlled at 120 °C. The level in the steam generator is controlled by the condensate return pump. Both the flue gas and the solvent entering the absorber tower are cooled to a temperature of 40 °C to keep the temperatures in the column low. These temperature are controlled via the cooling water flow of the corresponding coolers. The absorber sump level is controlled by the valve downstream the lean-rich heat exchanger. As the level of the stripper sump is not controlled, this level is free to vary depending on operating conditions. When the water balance in the system is not in equilibrium, this level will not remain constant. Water entering and leaving the system can be regulated by controlling the temperatures of the streams leaving and entering the capture unit, namely the clean gas exiting the absorber and the CO_2 flow exiting the stripper. During normal operation the temperature of the flue gas entering the absorber and the CO_2 product flow are controlled at a constant value. The temperature of the washing section is then adjusted to maintain a constant amount of water in the system. It is necessary to maintain the water balance to keep the solvent strength at 30 wt%. See Table 2-1 for the normal operating conditions and Table 2-2 for the controlled and manipulated variables of the pilot plant.

Table 2-2: Controlled and manipulated variables of the capture pilot plant

Controlled variable	Manipulated variable
Flue gas flow	Flue gas valve opening
Solvent flow	Lean solvent valve opening
Absorber level	Rich solvent valve opening
Lean solvent temperature	Lean solvent cooling water valve opening
Caustic solution temperature	Caustic solution cooling water valve opening
Clean gas temperature	Wash water cooling water valve opening
Stripper pressure	CO_2 product valve opening
Reboiler temperature	Steam valve opening
Stripper condensate tank level	Stripper condensate pump speed
Steam generator level	Steam generator condensate pump speed

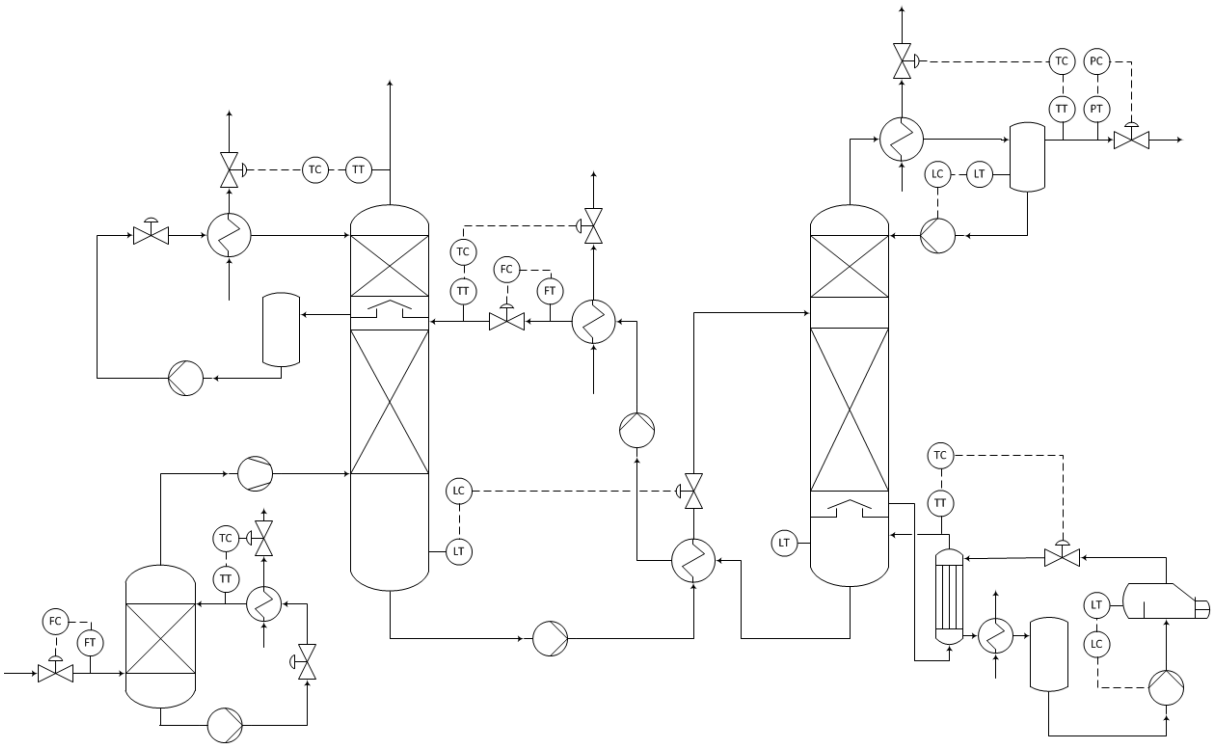

Figure 2-3: A simplified P&ID of the capture pilot plant

Chapter 3

Model development

This chapter describes the development of the dynamic model. First, an existing steady-state model developed by TNO is improved and modified to the specific operational conditions of the pilot capture plant. Then, with the steady-state model as a basis the dynamic model is developed. This is done by using and adapting existing Modelica libraries.

3-1 Steady-state model development

Steady-state performance models are commonly used for design, analysis and optimization of processes. In this study, the steady-state model is used to provide initial values for process variables in order to ease the initialization process of dynamic simulations.

3-1-1 Model description

For steady-state simulation of the capture unit a common, commercial software tool[30] dedicated for the modeling of chemical processes has been used. The individual components of the capture unit have been modelled using models from the component library of the process simulator. For the absorber and stripper the RadFrac column model has been selected. For the chemistry and thermodynamics in the column an equilibrium or rate-based approach can be chosen. Although a rate-based approach gives a more accurate representation of the column[24], for simplicity the equilibrium-based approach has been chosen. To model the absorption process in the column, the column has been discretized into a number of stages. A higher number of stages results in a higher accuracy but also increases the computational simulation time. In order to determine the required discretization, the absorber has been modeled for different number of stages varying from 3 to 50. The capture rate increases for an increasing number of stages (see Figure 3-1). Above 20 stages the solution in terms of capture rate does not change significantly any more and therefore, this number of stages has been chosen for the absorber.
The simulation tool provides different electrolyte-based chemistry models such as EMEA, KEMEA, MEA and KMEA that provide the chemistry properties for the monoethanolamine (MEA) based solvent. These packages use the electrolyte non-random two-liquid(NRTL)

method, which is an activity coefficient model-based property method to model the thermodynamic properties. It uses the electrolyte NRTL model for the liquid phase and the Redlich-Kwong equation of state for the vapour phase. For the modeling of the MEA solvent the KEMEA chemistry model is suggested by the user guide of the software [31] for systems with temperatures up to 120 °C. See Table 3-1 for the selected component models and methods. Due to limitations in the available component models, the system to be modeled had to be simplified. The software tool does not support the modeling of a separate reboiler and therefore the bottom stage of the stripper is modeled as a reboiler with a specified heat duty.

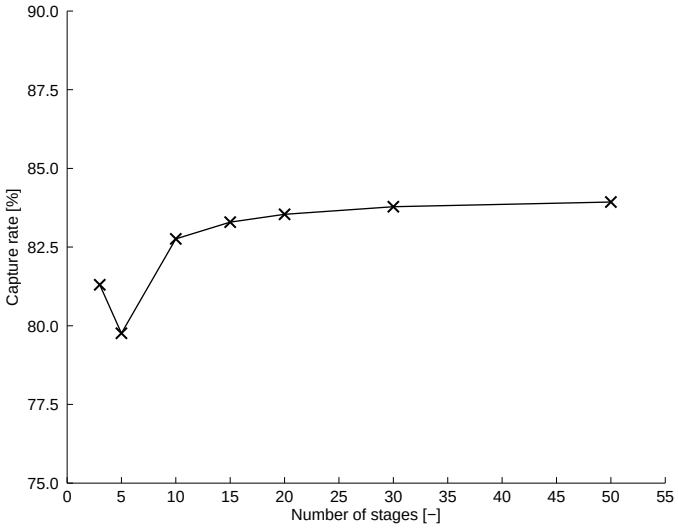

Figure 3-1: The capture rate for a different number of stages in the steady-state absorber model

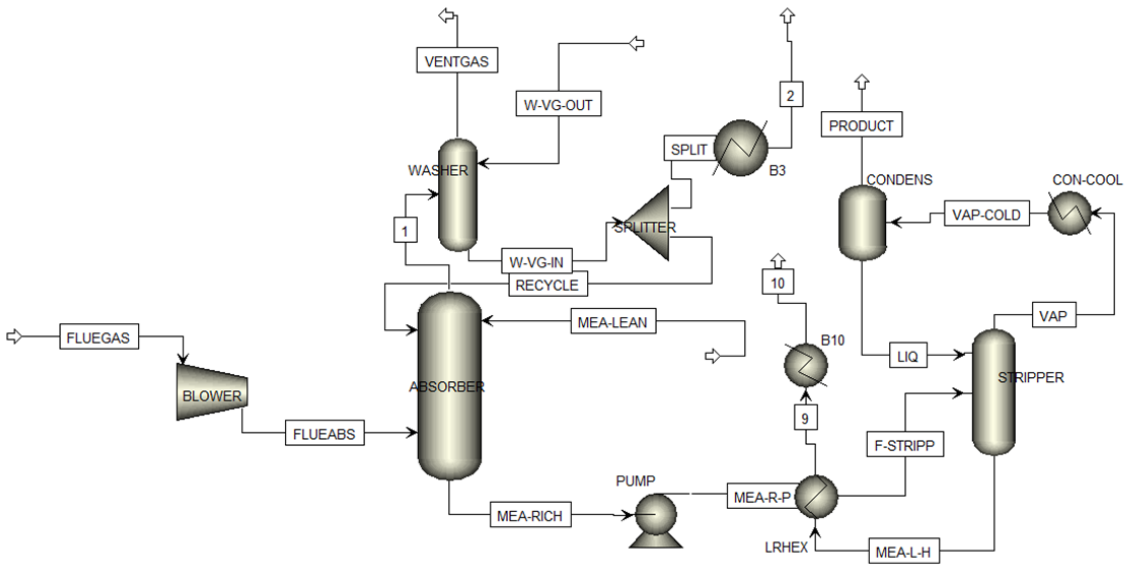

Figure 3-2: Process flow diagram of the steady-state model of the CO_2 capture unit in the steady-state software tool

Table 3-1: Input selections, parameters and variables for the steady-state model of the CO_2 capture unit

Description	Value/selection
Absorber	
Model type	RadFrac
Calculation mode	Equilibrium
Convergence algorithm	Strongly non-ideal liquid
Top stage pressure	1.01 bar
number of equilibrium stages	20
Column pressure drop	0.05 bar
Desorber	
Model type	RadFrac
Calculation mode	Equilibrium
Convergence algorithm	Strongly non-ideal liquid
Top stage pressure	1.9 bar
Number of equilibrium stages	9 (including reboiler stage)
Column pressure drop	0.02 bar
Other	
Flue gas flow	800 Nm^3/h
Flue gas composition (H_2O, O_2, CO_2, N_2)	0.074, 0.05, 0.137, 0.739
Lean solution flow	3.2 ton/h
Reboiler duty	140 kW
Wash water flow	1.2 ton/h
Stripper condenser temperature	25 °C
General	
Solution option	Sequential modular
Property method	ELECNRTL
Chemistry model	KEMEA

3-1-2 Model simulation and results

The lean solvent recycle stream makes the convergence of a simulation troublesome. In order to allow for good and fast convergence of the solution the solvent recycle is not closed. Hence, the outlet stream of the solvent cooler is not connected to the solvent inlet stream of the absorber (see Fig. 3-2). The correct steady-state solution is obtained by manual iteration, copying the results of the solvent cooler outlet stream to the input of the lean solvent inlet at the absorber till good agreement of both streams is reached.

Table 3-2: Comparison of the steady-state model results and capture pilot plant measurements

		Pilot plant measurements	Steady-state model
Reboiler temperature	[°C]	120	120
Capture rate	[%]	95.2	68.8
Rich loading	[mol/mol]	0.483	0.496
Lean loading	[mol/mol]	0.236	0.283

In order to obtain the same temperature as in the pilot plant the reboiler duty is adjusted. The wash water temperature is adjusted to keep the water balance. The simulation results based on the specified inputs (see Table 3-1) are listed in Table 3-2. The carbon dioxide (CO_2) capture rate is predicted by the model significantly lower compared to the pilot capture plant. One reason for the difference in CO_2 capture rate can be the difference in lean loading (5%-points lower in simulation). Further analysis of the CO_2 balance over the absorber indicates that it is very likely that one of the flow (flue gas or solvent) measurements are not correct. When comparing the temperature profile in the absorber in Figure 3-3 it can also be seen that the temperatures predicted by the model are much lower compared to the experiments, which is caused by the lower capture predicted rate in the model. Possible causes for the mismatch of the flow measurements are discussed in Chapter 4.

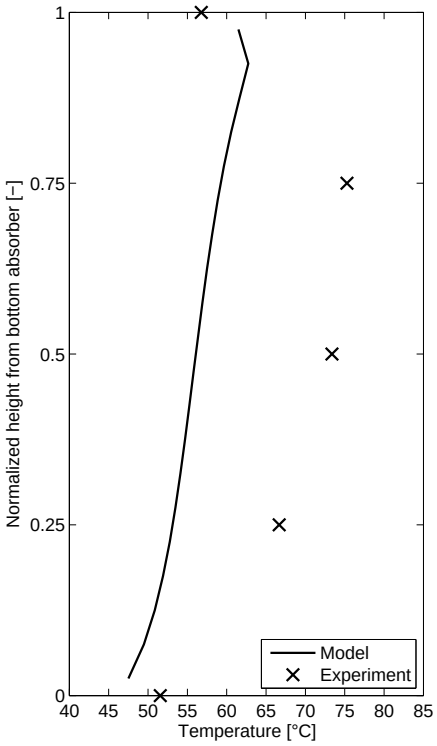

Figure 3-3: Comparison of steady-state model results and pilot capture plant measurements for absorber temperature profile

3-2 Dynamic model development

For the development of the dynamic model of the capture unit the following stepwise approach presented in Ref. [32] has been followed.

1. Purpose
2. System border and variables
3. Relevant phenomena
4. Hypotheses
5. Sub models
6. Conservation laws and relations
7. Simplification
8. Implementation and simulation
9. Validation, documentation and application

This modeling process is an iterative process, after simulation and validation of the process one might reconsider if chosen hypotheses are valid and if all relevant phenomena are considered. In this section steps one to five are described. Steps five, six and seven are clarified in appendix A. The simulation and validation part is described in Chapter 4. The application of the dynamic model is tested and documented in the Chapter 5.

3-2-1 Purpose of the model

The purpose of the dynamic model is to asses the dynamic responses of a capture plant for a coal-fired power plant during load variation. The analysis will be carried out with a dynamic model of only the capture unit applying meaningful boundary conditions in order to account for the interaction with the coal-fired power plant. As only load variation of the capture unit will be studied, fast dynamics are not of interest for this model.

3-2-2 System border and variables

The system border separates the system from its surrounding (see Figure 3-4). The boundary must be placed where there are some known inputs and/or wanted outputs. For the capture pilot plant there are known inputs at the flue gas inlet upstream the flue gas scrubber. The flue gas flow and its CO_2 composition at this position is measured. Furthermore, it is known that the pressure at the outlet of the washing section is close to atmospheric and the pressure at the outlet of the product cooler is measured and controlled. When looking at integration with the power plant, the steam inlet is a variable of interest since this has an impact on the operation of the steam turbines in the power plant. Inclusion of the steam generator and the condensate vessel is therefore not necessary.

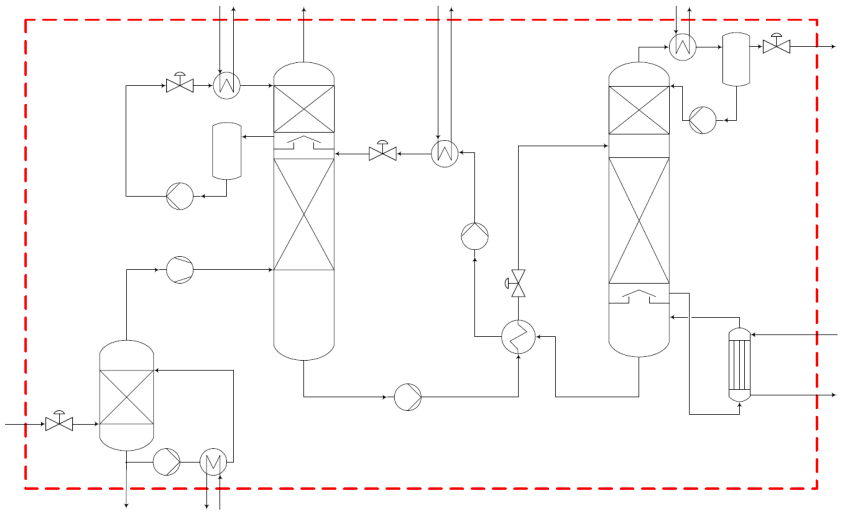

Figure 3-4: System border of the dynamic capture plant model

Table 3-3: General input and output variables for the dynamic capture plant model

Flue gas flow rate
Flue gas composition
Washing section outlet pressure
Clean gas flow
Clean gas composition
Clean gas temperature
Lean solvent cooling duty
Stripper outlet pressure
Reboiler heat duty
Product flow
Product composition
Product temperature
Condenser cooling duty

3-2-3 Relevant phenomena

In this step the relevant phenomena describing the performance of the system need to be identified following the principle of parsimony. This means that one should only model the necessary phenomena by deciding which phenomena are relevant and which negligible. The main relevant phenomena of the system are:

- Heat and mass transfer between the liquid and gas phase in the columns
- Chemical reaction in the liquid phase in the columns
- Convective heat transfer in the heat-transfer equipment
- Accumulation of mass and energy in the fluid flows in columns, heat exchangers and sumps
- Accumulation of thermal energy in heat exchanger plates and column packing material
- Frictional losses in columns, valves and heat exchangers

3-2-4 General hypotheses and assumptions

To simplify the modeling problem, suitable hypotheses and assumptions are made. The general hypotheses and assumptions to develop the model are listed below. The specific hypotheses and assumptions for each module can be found in the module descriptions in appendix A.

- The volume in the pipes and pumps is small compared to the other components and can be neglected (see Table 3-4)
- The pressure at the outlet of the absorber is constant as it is close to atmospheric
- The pressure at the outlet of the stripper is constant as it is controlled at a fixed pressure
- The composition and temperature of the flue gas entering the capture unit is constant as the load of the power plant is not changed during the tests
- The flue gas blower has a negligible influence on the system and can be therefore omitted
- The flow from the condensate tank at the stripper product gas outlet is small and its on/off flow control can be replaced by a continuous flow from the condenser
- MEA has a low volatility and therefore it is assumed that MEA is not present in the gas phase
- In the flue gas only carbon dioxide, oxygen, water and nitrogen are present
- In the product gas only carbon dioxide and water are present
- All components are well insulated and therefore heat loss the environment is negligible (adiabatic)

Table 3-4: Solvent hold-up in the capture pilot plant

Component	Volume [L]
Absorber packing[1]	72
Absorber sump	1272
Stripper packing[1]	56
Stripper sump	770
Rich/lean heat exchanger	69
Lean solvent cooler	11
Piping	253
Pumps	5
Total	2508

3-2-5 Subsystems

The model is developed following the causality principle which means, that bilaterally coupled variables, such as for example pressure and flow rate, are not imposed at the same boundary. This ensures that the index of the resulting mathematical problem is one and therefore the solution can be easier obtained by the numerical solver. As described in Section 1-1-3 in the causal modeling two basic types of modules are used, resistive and storage modules. In order to follow the causality principle resistive modules should only be connected to storage modules and vice versa. This approach forces the modeller to sometimes choose an other structure than identified according to the relevant phenomena. In case of the dynamic model

[1] Estimated with the steady state model

of the pilot plant, an example is the rich solvent side exiting the absorber (see Figure 3-6). As the rich solvent pump upstream and the valve downstream the lean-rich heat exchanger are resistive components, the rich solvent side of the lean-rich heat exchanger should be modelled with a storage component. Hence, the resistive phenomena related to frictional losses should be lumped in either the model of the rich solvent pump or the valve. For every component, the causality structure is described in detail in Appendix A.
The decomposition of the model into subsystems allows to better manage the complexity of the model and further enables the re-use of modules. The complete system is divided into components which are further decomposed into reusable sub modules. Each system component is modelled with a suitable dynamic model taken from either the ThermalSeparation or ThermoPower library. Where necessary, the models were adapted to the specific requirements of the pilot plant components. This subsection provides an overview over the selected models with their sub modules and parameter values. The result of the applied assumptions to the structure of the dynamic model can be found in Figure 3-5.

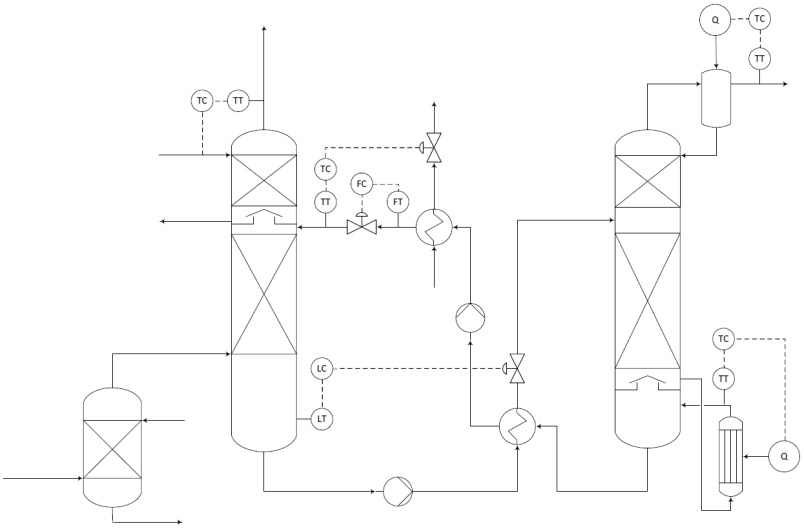

Figure 3-5: P&ID diagram with the structure of the complete dynamic model

Flue gas scrubber, absorber and washing section

The flue gas scrubber has two purposes, cooling of the flue gas and removal of SO_2. As the presence of SO_2 in the flue gas has a negligible influence on the dynamic performance of the capture plant it can be assumed that the flue gas scrubber removes all SO_2 present. Therefore it is assumed that in the gas medium only H_2O, O_2, CO_2 and N_2 are present. As the inlet temperature of the scrub solution is controlled at a constant temperature, its input variable is fixed.
The four random-packed beds in the absorber column are modeled as one bed with a height equal to the total height of the four beds. For the flue gas scrubber, absorber and washing section the packed column model from the ThermalSeparation library as described in Appendix A-1 has been used. For all components the Stichlmair pressure drop and hold-up correlations are used as these correlations are well known and have been validated against experimental data.
For simplicity and to avoid switching to another media model, the liquid medium in the washing section is modelled with the H_2O-CO_2-MEA media model. All accumulated water in the washing section is returned to the absorber which is modeled with a splitter.

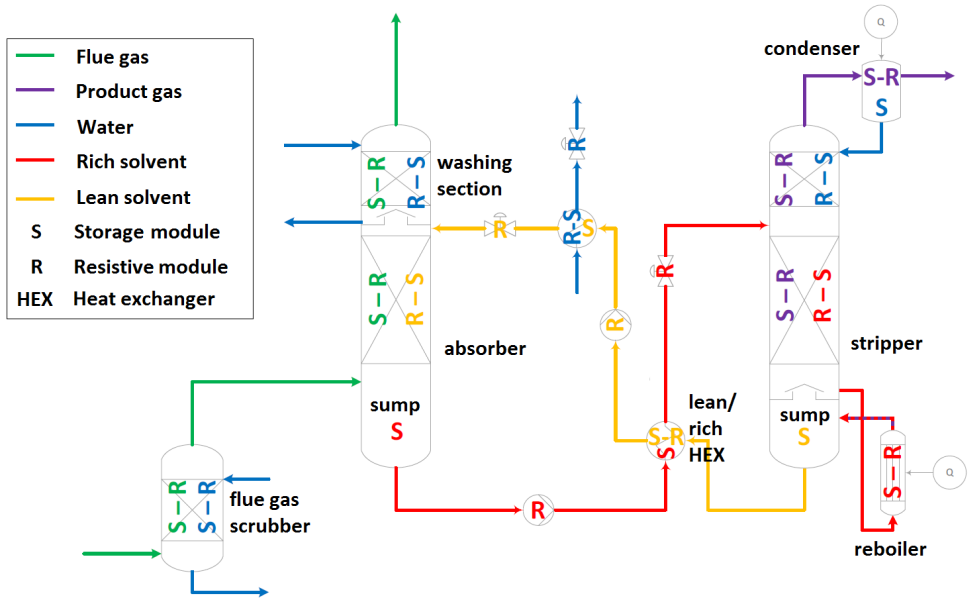

Figure 3-6: Causality diagram of the complete dynamic model

Table 3-5: Sub model selection and parameter values for the column components in the dynamic model of the capture unit

	Flue gas scrubber	Absorber	Washing section	Stripper
Model	Packed column			
Vapour medium	H_2O, O_2, CO_2, N_2			H_2O, CO_2
inertVapour	false, true, false, true			false, false
Liquid medium	H_2O, CO_2, MEA			
inertLiquid	false, false, true			
Pressure loss correlation	Stichlmair			
Hold-up correlation	Stichlmair			
Heat loss to environment	No (adiabatic)			
Film model	true equilibrium			
Metal heat capacity [J/(kg.K)]	460			
Metal density [kg/m^3]	7900			
Number of stages	5	20	5	5
Diameter [m]	0.65	0.65	0.65	0.45
Height [m]	2.0	8.4	2.0	8.2
Void fraction	0.98			
Specific area [m^2/m^3]	102	102	256	102
1st Stichlmair constant	0.8821114		1.0	0.8821114
2nd Stichlmair constant	-0.0831108		1.0	-0.0831108
3rd Stichlmair constant	1.143401		0.32	1.143401

Stripper and reboiler

The reboiler is modelled with the reboiler model taken from the ThermalSeparation library. The reboiler is modelled as a single equilibrium stage whereby the amount of liquid hold-up is calculated based on the vapour quality in equilibrium condition. This simplification results in unrealistically low liquid contents in the reboiler. In order to obtain more realistic liquid hold-up, the reboiler dimensions and the number of tubes are increased (see Table 3-6).

Table 3-6: Sub model selection and parameter values for the reboiler component in the dynamic model

Vapour medium	H_2O, CO_2
inertVapour	false, false
Liquid medium	H_2O, CO_2, MEA
inertLiquid	false, false, true
Tube diameter [m]	0.025
Tube lenght [m]	10
Number of tubes	450

Sumps

The system contains two sump components, one absorber and one stripper sump. It is assumed that the sumps are ideally mixed, no reactions take place in the sumps and that no heat is lost to the environment. The dimensions of the sumps are the same as of the sumps in the capture pilot plant (see Table 3-7).

Table 3-7: Sub model selection and parameter values for the sump components in the dynamic capture plant model

	Absorber sump	**Stripper sump**
Vapour medium	H_2O, O_2, CO_2, N_2	H_2O, CO_2
Liquid medium	H_2O, CO_2, MEA	
Diameter [m]	0.9	0.7

Heat exchangers

The heat exchangers are modeled with tubular heat exchanger models taken from the ThermoPower library. Although the heat exchangers in the capture pilot plant are plate heat exchangers, the models can be used by adjusting the volume and heat transfer area to the dimensions of plate heat exchangers. The models are adapted in terms of their media model and connectors. Depending on the causality scheme, the pressure drop is whether or not accounted for. The heat transfer coefficient is a parameter of which the fitting is described in Chapter 4.

Table 3-8: Sub model selection and parameter values for the heat exchanger components in the dynamic model

		Lean-rich heat exchanger	**Lean solvent cooler**
Model		Heat exchanger	
Medium side 1		H_2O, CO_2, MEA	
Medium side 2		H_2O, CO_2, MEA	H_2O, CO_2
Fluid volume side 1	[L]	34.5	11
Fluid volume side 2	[L]	34.5	11
Metal volume	[L]	14.75	5
Metal specific heat capacity	[J/(kg.K)]	460	
Metal density	[kg/m^3]	7900	
Heat exchange surface	[m^2]	29.5	10
Nominal flow rate side 1	[kg/s]	2.6	2.6
Nominal flow rate side 2	[kg/s]	2.6	8.0
Nominal pressure drop side 1	[bar]	0.4	0.4
Nominal pressure drop side 2	[bar]	0.4	0.5

Pumps

For the pumps, models from the ThermoPower library are used. Required are a curve for the pump head and power. For the head curve and the power curve three nominal operating points are taken from vendor specifications. It is assumed that these pumps run at nominal speed.

Table 3-9: Sub model selection and parameter values for the pump components in the dynamic model

		Lean solvent pump	**Rich solvent pump**
Model		Pump	
Flow characteristic		Quadratic	
Power characteristic		Quadratic	
Flow values for head curve	[m^3/s]	0, 0.0025 ,0.0033	
Head values for head curve	[m]	47.6, 42.4, 39.3	
Flow values for power curve	[m^3/s]	0, 0.0021, 0.0028	
Power values for power curve	[W]	1685, 2285, 2445	

Valves

A number of valves have been eliminated from the model due to the applied simplifications. For the remaining valves the required parameter is the flow coefficient Kv, this is taken from manufacturers specifications and dependent on the valve size. These flow coefficients are listed in Table 3-10.

Table 3-10: Sub model selection and parameter values for the valve components in the dynamic model

	Lean solvent valve	**Rich solvent valve**	**Lean solvent cooling valve**
Module	Valve		
Flow characteristic	Equal percentage		
Flow coefficient Kv [m^3/h]	15	22.2	22.2

Controllers

In the capture pilot plant at the Maasvlakte only PI-controllers are used. For model validation the same control scheme and controller settings as present in the pilot are implemented in the model. However, due to simplifications it was required to introduce controllers which are not present in the capture pilot plant. These are the reboiler temperature controller, the condenser temperature controller and the washing section outlet temperature controller. For this new controllers the IMC-based controller settings presented in Ref. [33] are used to tune the controllers. The process reaction curve method has been used as this requires only a single open-loop step response test for tuning. A step on the manipulated control variable results in a reaction of the process variable. Based on this step response, the time constant τ and the process gain k of the process can be determined (see Figure 3-7). A diagram of the step response can be found in Figure A-7 to A-9 in appendix A-10. It can be seen that both responses can be approximated as a first-order system. Then, based on this results the PID settings of the controllers can be determined(see Tab.3-11). The variable τ_c is a variable which can be tuned by the user and as proposed by Ref. [34] it has been set to 1/3 of the process time constant τ.
A D-action is only required for processes with large dead times (larger than 30 seconds)[34]. Based on the process reaction curves it can be concluded that this is not the case in this capture unit, and therefore PI-controllers are sufficient (see Fig.3-12).

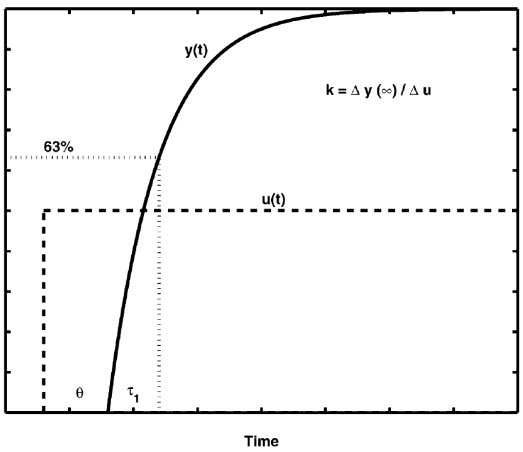

Figure 3-7: Step response of a first-order plus time delay process [35]

Table 3-11: IMC-based PID controller settings for a first-order model

K_c	τ_I	τ_D
$\frac{\tau}{k\tau_c}$	τ	-

Table 3-12: PID controller settings in the dynamic model of the capture pilot plant

Controller	K_c (normalized)	τ_I
Lean solvent flow	2	20
Absorber level	-2	240
Lean solvent temperature	-1	10
Reboiler temperature[1]	10	200
Condenser temperature	-0.40687	3.3
Washing section outlet temperature	2.94	12.48

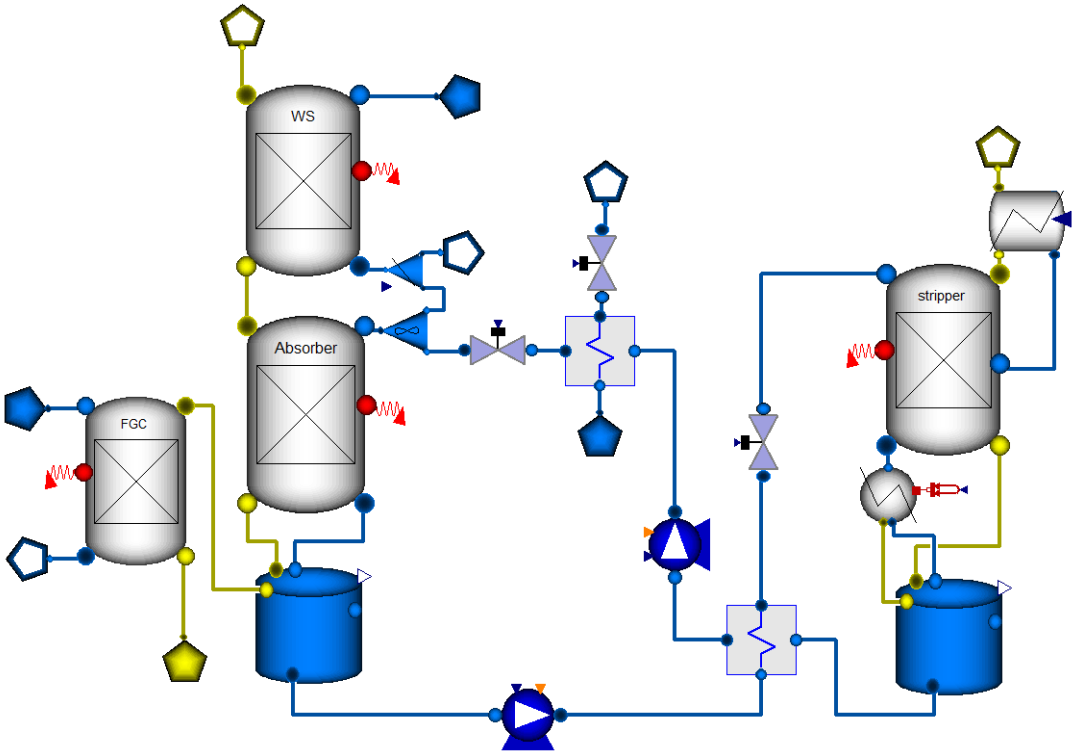

Figure 3-8: Complete dynamic model of the pilot capture plant

[1]The reboiler controller PID settings are adjusted to match the performance of the reboiler as observed in validation test B1 (see also Section 4-4).

Chapter 4

Model validation

Model validation is a key step of the model development procedure demonstrating the agreement between simulation results and literature or experimental data of the system modelled. Especially the model validation against experimental process results will increase the reliability and confidence in the developed model. According to a test plan, open-loop step response test were performed at the capture pilot plant. First, unknown model parameters were fitted by matching steady-state model performance with experimental data. Then, the dynamic model validation was carried out by comparing the dynamic response of the main process variables for the model and experiments.

4-1 Test plan

In order to obtain experimental data for transient operation of the capture unit, open-loop step tests were performed. During common operational scenarios such as ramping the flue gas flow and the solvent flow are the most important variables which undergo changes. If the flue gas flow increases or decreases due to load variations in the main power plant, then the solvent flow has to adjust in order to maintain a low specific energy demand and to keep an optimal liquid-to-gas (L/G) ratio in the absorber. Therefore, these two variables have been chosen as perturbation variables for the experimental tests. During the tests the flue gas and solvent flow controller are operated in manual mode in order to observe the system response without masking control actions. In general, the applied perturbation should be large enough such that a clear system response can be observed which is larger than signal noise but does not exceed the plant capacity limitations. Based on the operational limits of the capture pilot plant four different step tests were performed (see Table 4-1), two in which the flue gas flow is changed (case A1 and A2) and two in which the solvent flow is changed (case B1 and B2). All other controller set points remained unchanged during these tests. The tests were performed on November 5, 2012 at the capture pilot plant.
For a solvent flow of 3.2 ton/h and a total liquid inventory of 2600 L the residence time of the liquid is approximately 50 minutes. Therefore the time between two tests is at least two hours to have sufficient time to let the system stabilize and reach steady-state. During the tests this time guideline and the actual on-line measurements have been used to identify if steady-state operation is reached and the next perturbation can be applied.

Table 4-1: Overview of open-loop capture pilot plant step tests for flue gas and solvent flow perturbations. For every test the perturbed variable is highlighted in bold.

	Solvent flow [ton/h]	Flue gas flow [m^3/h]	Stripper pressure [bar]
Normal operation	3.2	800	1.9
Test A1	3.2	**580**	1.9
Test A2	3.2	**800**	1.9
Test B1[1]	**4.4**	800	1.9
Test B2[1]	**3.2**	800	1.9

4-2 Validation variables

Changing the L/G ratio in the absorber affects the capture rate of the pilot plant. A higher L/G ratio will result in a higher capture rate and vice versa. Due to the exothermic absorption reaction, a change in capture will also affect the absorber temperature profile. Therefore, the absorber temperatures are appropriate variables for dynamic validation of the model. Temperature changes have also a large influence on the dynamics of the other downstream processes such as heat exchangers, the reboiler and the stripper. Therefore the top and bottom temperatures of the absorber are chosen for the comparison of response. Since the stripper pressure and the reboiler temperature remain unchanged during the experiments, it is expected that the vapour and liquid composition exiting the stripper will remain constant as well. For the dynamic validation of solvent properties, the solvent is sampled during the experiments at the absorber and stripper sump. Both the monoethanolamine (MEA) and the CO_2 concentration are required measurements to determine CO_2 loading of the solvent. The MEA concentration together with the density is measured in order to determine the solvent weight fraction. It can be assumed that the solvent concentration is constant during the experiments, as MEA is non-volatile and the accumulation of water is negligible. Therefore, it is only measured before the perturbation (at time= -10min). During the first half hour after a perturbation the solvent is sampled every ten minutes since in this period the highest change is expected (See Table 4-2).

Table 4-2: The sampling plan for solvent at the absorber and stripper sump during the experiment. The highlighted properties will be evaluated.

Sample time [min]	CO_2 [mol/l]	MEA [mol/l]	Density [kg/m^3]
-10	x	x	x
0[2]	x		
10	x		
20	x		
30	x		
60	x		
120	x		

[1]Due to failure of a valve, test B1 was unsuccessful and only data of the first 30 minutes after the perturbation is usable. Due to the failure, test B2 could not be performed.

[2]At time instant 0 the perturbation is applied to the specified variable

4-3 Parameter fitting

In order to match the steady-state performance of the dynamic model with the capture pilot plant at the Maasvlakte, fitting of unknown parameters is necessary. Unknown parameters are the heat transfer coefficients in the lean-rich heat exchanger and the lean solvent cooler. These heat transfer coefficients are adjusted to match the outlet temperatures at nominal conditions. The results of the parameter fitting are listed in appendix B-3. A simulation has been performed with this fitted parameters and the steady-state results are summarized in the second column of table 4-3. One can observe that the rich and lean loadings do not match the ones in the capture pilot plant. The rich loading exiting the absorber is too high, and the lean loading too low. The mismatch in rich loading can be explained by the fact that in the model equilibrium is assumed which in practice commonly not is reached. In order to account for deviations from equilibrium conditions, a calibration factor (factor_K) in the media model can be adjusted. The equilibrium constant in the absorber is adjusted to match the loading of the rich solvent exiting the absorber before perturbation. The mismatch in lean solvent loading can be resolved by either an increase of the reboiler temperature or a reduction of the stripper pressure. As the last one has the least impact on other connected process units, a reduction of the stripper pressure has been chosen. With this proposed fitting there still remains a mismatch in steady-state values of the capture rate and the absorber temperatures as also already noticed during steady-state model development. This mismatch is very likely to be caused by incorrect measurements of the flue gas or the solvent flow. The flue gas is measured as well upstream as downstream the flue gas cooler, and the solvent both at the inlet and the outlet of the absorber. This makes it difficult to point out which measurement is incorrect. During the experiments it has been observed that the blower is leaking flue gas at high flows. Therefore the mismatch is very likely to be caused by biased measurements or a leakage of flue gas after the measurement location. To get the same steady-state capture rate as in the pilot plant, the flue gas flow is adjusted (see Table 4-3).

Table 4-3: Comparison of steady-state model results for the case of unfitted and fitted model parameters with capture pilot plant measurements

		Pilot plant measure-ments	Model (unfitted)	Model (fitted)
Flue gas flow	[Nm^3/h]	800	800	640
Lean solvent flow	[ton/h]	3.2	3.2	3.2
L/G ratio	[kg/kg]	3.0	3.0	3.7
Stripper pressure	[bar]	1.90	1.90	1.83
Reboiler temperature	[$^\circ$C]	120	120	120
Capture rate	[%]	95.2	83.0	95.1
Rich loading	[mol/mol]	0.483	0.550	0.482
Lean loading	[mol/mol]	0.236	0.272	0.236
Calibration factor (factor_K)	[-]	-	1.0	1.117

4-4 Validation results

The model validation has been performed by comparing the capture rate, absorber top and bottom temperatures, temperature profiles of the absorber column and carbon dioxide (CO_2) loading of the lean and rich solvent. The comparison of the simulation results for the tests A1,A2 and B1 with the experimental measurements for the mentioned variables is summarized in Figure 4-1 to 4-4. Since test B2 could not be performed, results for comparison of this test are not available.

Table 4-4: Test matrix of open-loop pilot plant test with corrected input variables. The original data as presented in table 4-1 is listed in brackets.

	Solvent flow [ton/h]	Flue gas flow [Nm^3/h]	Stripper pressure [bar]
Normal operation	3.2	640 (*800*)	1.83 (*1.9*)
Test A1	3.2	**555** (*580*)	1.83 (*1.9*)
Test A2	3.2	**640** (*800*)	1.83 (*1.9*)
Test B1	**3.7** (*4.4*)	800	1.83 (*1.9*)
Test B2	**3.2**	800	1.83 (*1.9*)

From Figure 4-1(c) it can be observed that the steady-states of the capture rate before and after the perturbation match well. This is a result of the parameter fitting and the correction of the measurements as described in section 4-3. Though, unstable operation of the steam generator causes a temporary decrease in capture rate at time -20, 20, 60 and 105 minutes. This period changes in capture rate is not predicted by the simulation as the steam generator is not modelled. The transient response of the capture rate is predicted slightly faster in the model than observed in the pilot plant. This could be due to that the gas volumes in between the beds are not modeled which would cause the slower response of the capture rate. Secondly, this could be caused by the assumption that the reactions in the absorber are in equilibrium, which would result in a prediction of a much faster response than observed in the experiments. From the comparison of the absorber temperatures depicted in Figure 4-1(d) it can first be observed that the steady-states do not match exactly. This can be caused by an incorrect prediction of the heat of absorption, and an other distribution of the capture throughout the absorber column. Considering the transient response of the absorber top and bottom temperature a good agreement with the experiments can been seen. Due to the step decrease in flue gas flow the L/G ratio in the absorber increases meaning that less CO_2 enters the absorber at the same solvent flow. The lower amount of CO_2 will already be absorbed at the lower part of the absorber column and as the absorption is an exothermic process the bottom temperature increases and the top temperature decreases. Because of this higher bottom temperature, the absorber sump temperature will also increase. This increase occurs abruptly in the experiment, whereas the model predicts a more gradual increase. This difference is caused by the fact that the sumps are assumed to be ideal-mixed, this assumption apparently does not hold. The rich loading is decreasing due the step in flue gas flow reaching steady-state after approx. 60 minutes. This transient is predicted well by the model. Though, the steady-state value after the perturbation is possibly overpredicted just fitting within the measurement accuracy. The lean loading remains constant as the stripper pressure and temperature do not change. In Figure 4-4(a-d) the absorber temperature profiles are compared.

Although the temperature profiles of both the model and the experiment show an increase, it can be observed that this increase is not evenly distributed. This might point out an error in the prediction of the heat of absorption and the distribution of CO_2 capture over the column.

Figure 4-2 depicts the comparison of experimental and model results for test A2 whereby the flue gas flow rate was increased stepwise. This is the same as in test A1 but with a reversed step, hence a similar, but reversed response is expected. As expected, the capture rate will decrease due to the lower L/G ratio and its steady-state value is the same as before the first perturbation. The predicted transient of the CO_2 capture rate matches well with the experimental measurements considering that the fluctuations induced by the reboiler are not captured by the model. Also the absorber temperatures in figure 4-2(d) show matching transients, but the offset in steady-state values remain.

The experimental results together with the model prediction of test B1, where the solvent flow rate was increased stepwise, is depicted in Figure 4-3. Experimental results for only the first 30 minutes after the perturbation are available which are nevertheless considered to be valuable for model validation. This test run is similar to a test A1 (flue gas decrease) as L/G will increase, therefore similar response is expected. The initial increase in capture rate is followed by temporary decrease in capture rate (t=10 minutes) which is caused by a delayed response of the reboiler. The sudden increased solvent flow will cause the reboiler temperature to decrease temporarily. These results were not observed with the initial IMC-based PID settings of the reboiler controller. Therefore, the controller settings are adjusted to observe a similar response. The sudden decrease in reboiler temperature can also be observed in the lean loading (figure 4-3f). A lower reboiler temperature results in a higher lean loading and thus a lower capture rate. These changes in capture rate due to the changes in reboiler temperature are predicted well by the model. For the absorber temperatures similar initial fluctuations are observed which are in terms of the transient in good agreement with the model predictions. However the height of the drop is smaller than predicted for the capture rate and the absorber temperatures. This could be due to the fact that the liquid is ideally mixed in the sump, resulting in a less abrupt impact on lean loading, capture rate and absorber temperatures. The other responses in figure 4-3 show the same trends as the ones in test A1, in which the change in L/G ratio is the same.

To summarize, for the executed test runs (flue gas flow increase and decrease, solvent flow increase) the transient responses in terms of trend and time constant for the capture rate, absorber temperatures, lean and rich solvent loading are in good agreement with the simulation results. Therefore, it can be concluded that the model can correctly predict the transient performance of the CO_2 capture pilot plant. Considering the steady-state predictions, mismatches are observed in temperatures and solvent loading. Possible explanations are biased measurements, leakage of flue gas in the blower and an inaccurate prediction of the heat of absorption. Therefore, the accuracy of the measurements need to be improved by recalibration of the measurement devices of the flue gas and solvent flow. In addition, the accuracy of the solvent composition measurement should be increased by improving the measurement method.

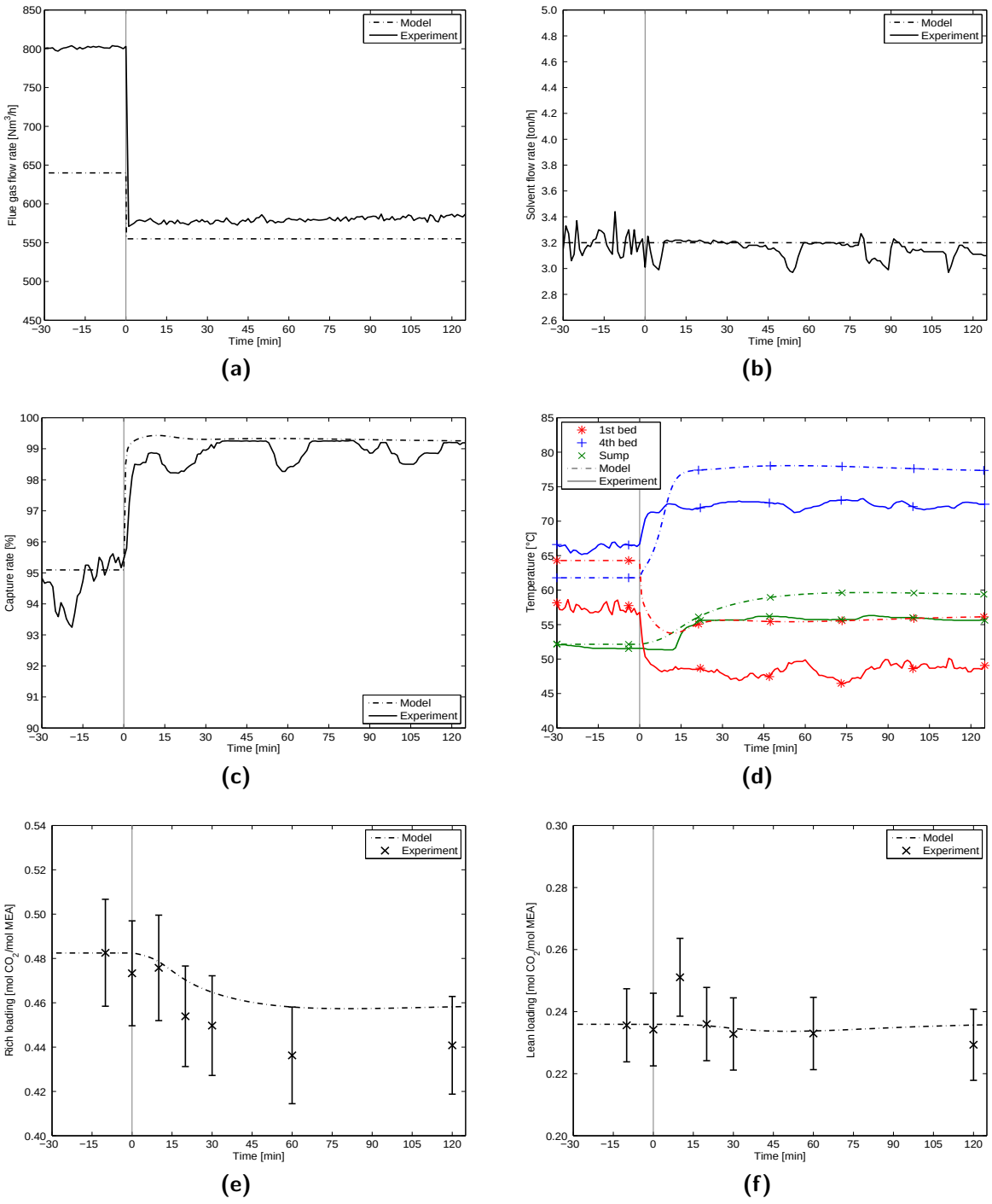

Figure 4-1: Comparison of open-loop step response of experimental data and model results for a step decrease in flue gas flow rate (test A1). Depicted variables are the flue gas flow rate (a), lean solvent flow rate (b), capture rate (c), absorber temperatures (d), rich solvent loading (e) and lean solvent loading (f)

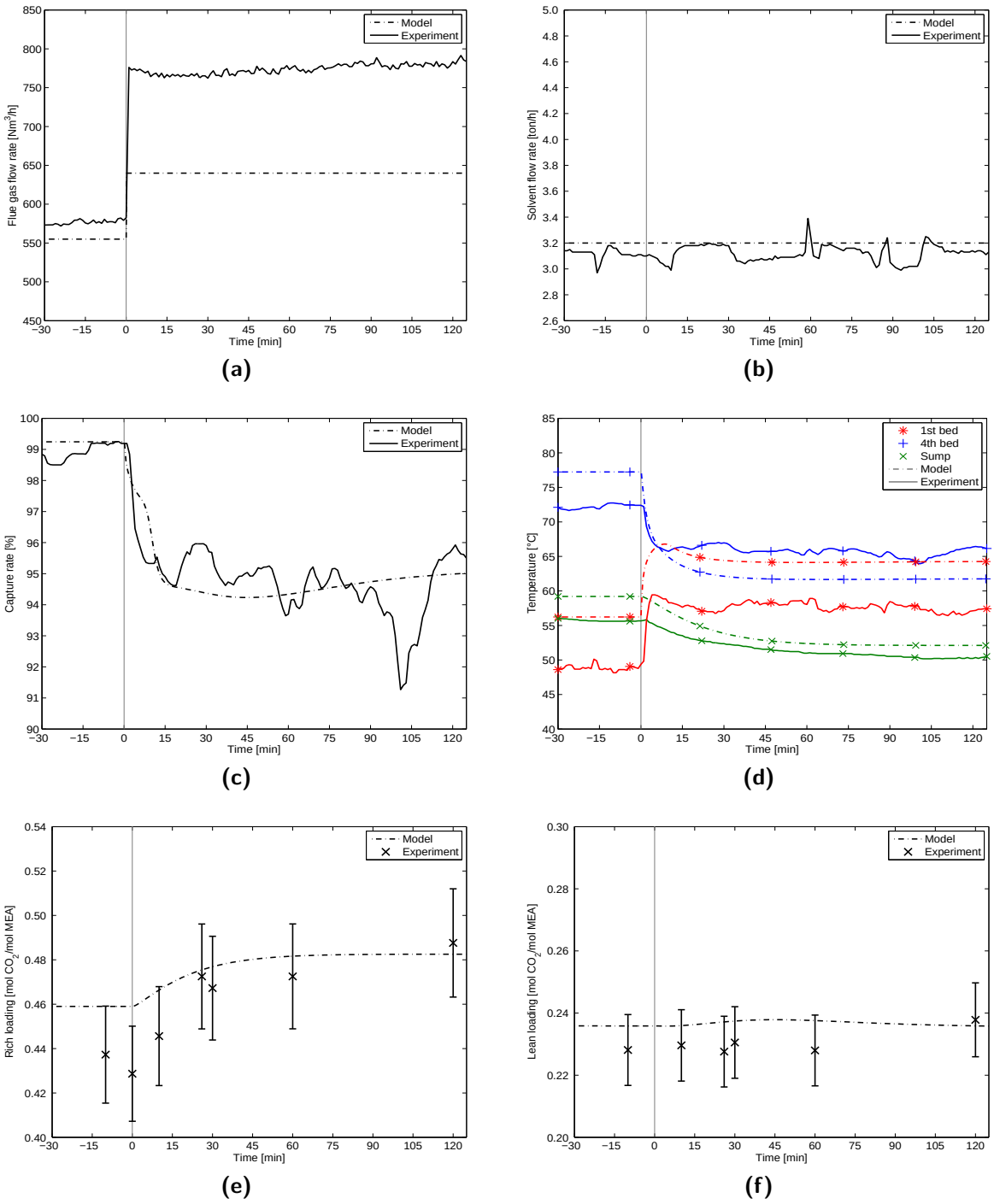

Figure 4-2: Comparison of open-loop step response of experimental data and model results for a step increase in flue gas flow rate (test A2). Depicted variables are the flue gas flow rate (a), lean solvent flow rate (b), capture rate (c), absorber temperatures (d), rich solvent loading (e) and lean solvent loading (f)

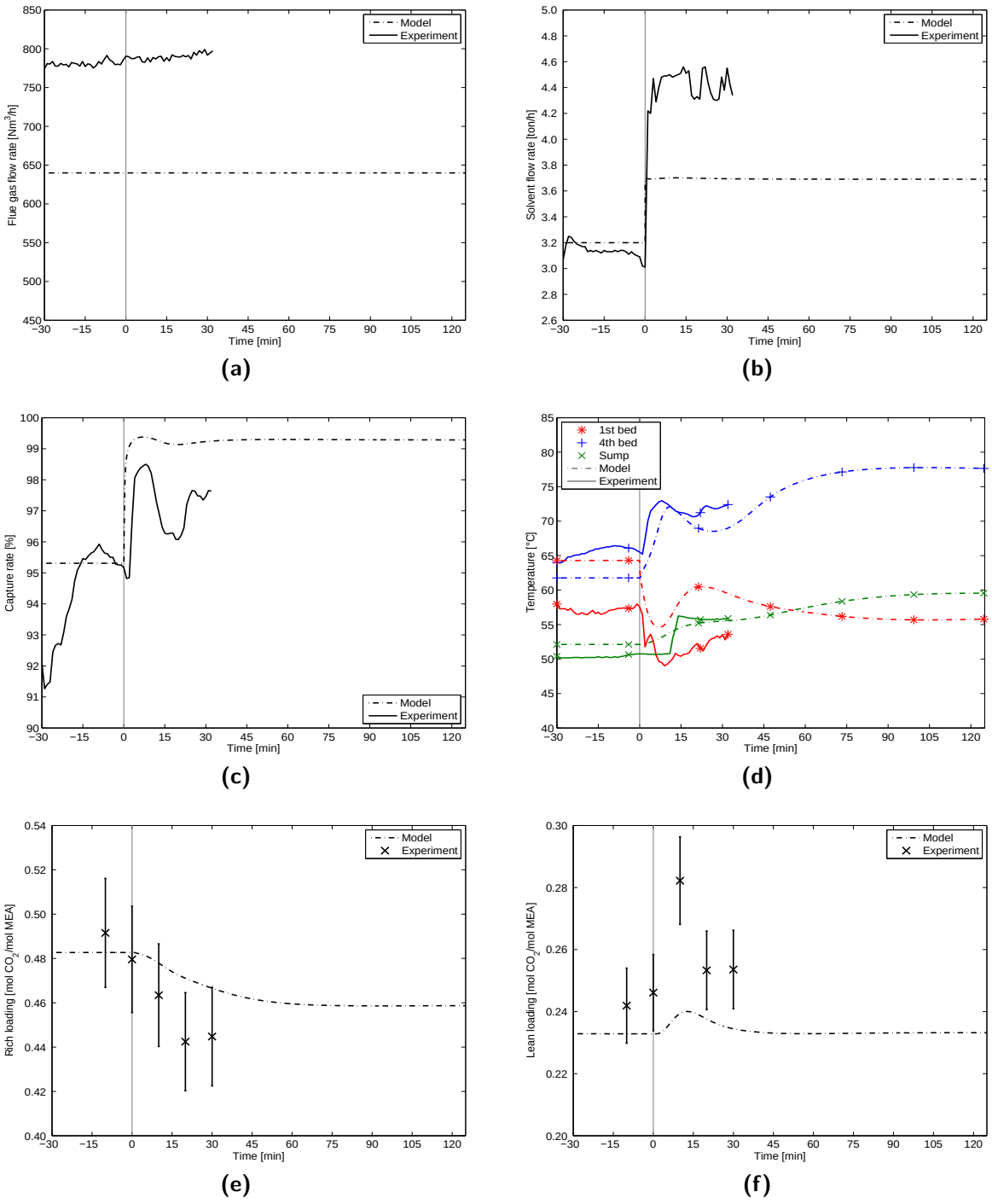

Figure 4-3: Comparison of open-loop step response of experimental data and model results for a step increase in the lean solvent flow rate (test B1). Depicted variables are the flue gas flow rate (a), lean solvent flow rate (b), capture rate (c), absorber temperatures (d), rich solvent loading (e) and lean solvent loading (f)

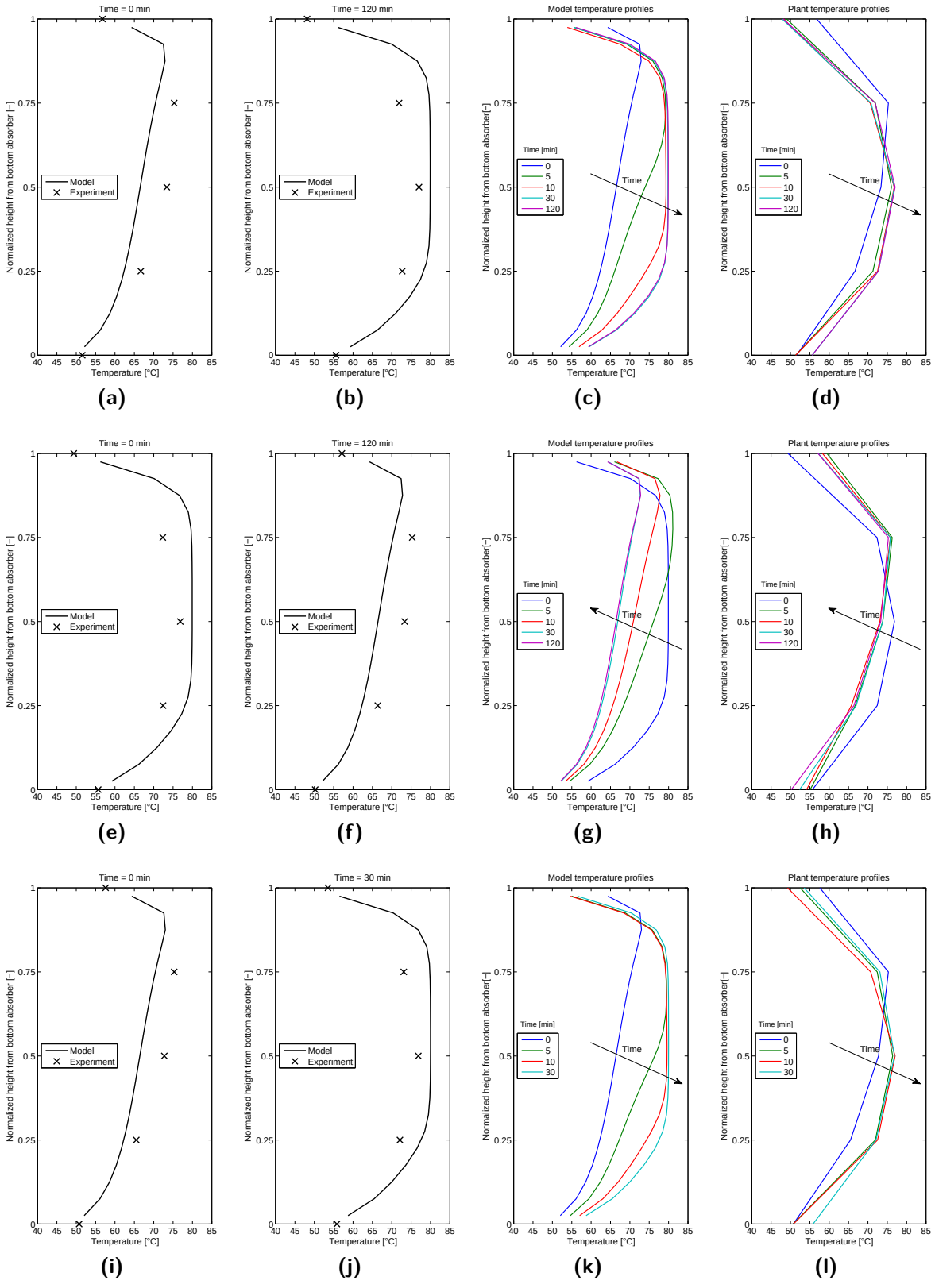

Figure 4-4: Comparison of the absorber temperature profiles of the model and the experiment for (a-d) a step increase of the flue gas flow rate (test A1), (e-h) a step decrease of the flue gas flow rate (test A2) and (i-l) a step increase of the lean solvent flow rate (test B1)

Chapter 5

Results

In this chapter, the dynamic performance of the pilot capture plant is analysed for three different load-variation scenarios of the coal-fired power plant. The analysis focuses on the transient of the capture unit and the streams which are connected to the power plant, namely the flue gas flow rate and the reboiler duty. A control structure allowing for load changes in capture unit has been proposed and implemented.

5-1 Proposed control structure

In the pilot plant the flue gas flow and the solvent flow are controlled separately which is required for the flexible execution of test runs. By adjusting the flows a desired capture rate can be obtained. For a large-scale capture unit it can be assumed that the entering flue gas flow is determined by the coal-fired power plant and that it is desirable to maintain a constant capture rate during operation to keep the temperatures in the absorber stable. This can be achieved by maintaining a constant liquid-to-gas(L/G) ratio in the absorber. Therefore, a ratio controller is proposed for the capture plant which controls the lean solvent flow rate in order to maintain a constant L/G ratio (see Figure 5-1). The measured flue gas flow is multiplied with the desired L/G ratio to determine the set point for the lean solvent flow controller.

5-2 Case description

In order to investigate the constraints and flexibilities during load variation of the power plant, three dynamic cases are defined. A common operational scenario of the main power plant is the load change from full load to part load and vice versa depending on the electricity price. This load change will result in a decrease of the flue gas flow entering the capture unit and subsequently in a period of transient performance in order to adapt to the new operational conditions. In the daytime there is a larger electricity demand and therefore the power plant is usually operated in full load. At night, the power plant load is reduced to its lowest possible load. This minimum load is usually 40% of the capacity for a coal-fired power plant. In the test cases the flue gas flow is decreased (case A) and increased (case B)

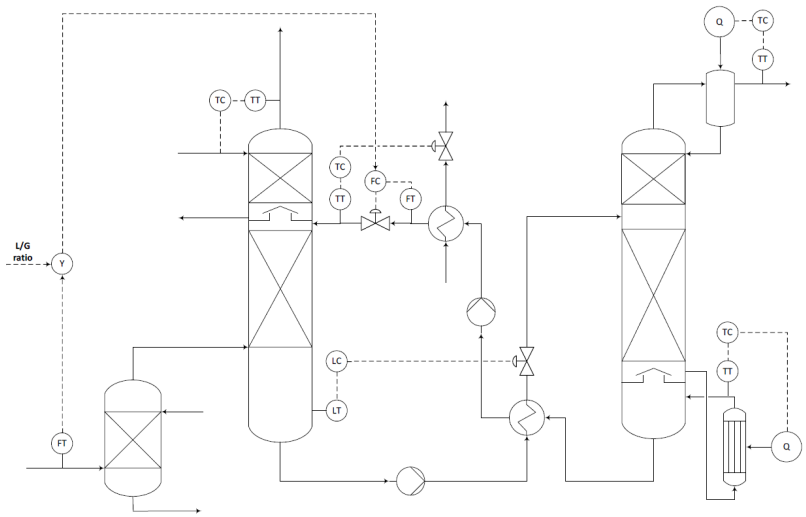

Figure 5-1: P&ID of the proposed control structure for the dynamic test cases

to monitor its dynamic response to this perturbation (see Table 5-1). Finally, a decrease in flue gas flow directly followed by an increase in flue gas flow is investigated (case C). This situation would occur if the power plant is operated more flexible due to more fluctuating electricity prices in day time. For all cases, a ramp rate of 4%/minute is assumed as this is a common ramping rate of a coal fired power plant. All other parameters and variables will be kept constant during these tests. Full load is assumed to correspond to the design load of the capture pilot plant(1500 Nm^3/h). The L/G ratio in the absorber was chosen to 3.6 kg solvent per kg of flue gas in order to achieve a CO_2 capture rate of 90% at nominal operation.

Table 5-1: Description of the three dynamic cases which will be tested with the model

Case A:	A decrease in flue gas flow rate. The flue gas flow rate will decrease from 100% to 40% with a rate of 4% per minute.
Case B:	An increase in flue gas flow rate. The flue gas flow rate will increase from 40% to 100% with a rate of 4% per minute.
Case C:	Temporary decrease in flue gas flow rate. The flue gas flow rate will decrease from 100% to 40% with a rate of 4% per minute and immediately increase to 100% at the same rate.

5-3 Case results

To assess the dynamic performance of the capture plant integrated with a power plant and downstream equipment such as the compressor train, one should investigate the response of relevant variables. For integration with the power plant, the reboiler heat duty is the variable to monitor as it determines the required extraction steam flow. For downstream processes the CO_2 product flow is relevant to study as the gas flow has a large influence on the compressor train operation. For the dynamic performance of the capture plant itself the CO_2 loading of the lean and rich solvent, the capture rate and the stripper level are monitored to check the system performance. The stripper sump level indicates if the water balances of the capture unit is stable.

The system response to case A (see Figure 5-2) shows that the capture rate stabilized after an initial increase direct after the perturbation. As expected, the capture rate remained approximately constant as the L/G ratio in the absorber was kept constant. The slightly increased capture rate is the result of a lower pressure drop in the stripper column due to a lower product gas flow. This causes a slightly lower lean loading and this therefore results in a slightly higher capture rate (see also Table 5-2). The stripper sump level (see Figure 5-2c) increases as the liquid hold-up of solvent in the packing of the absorber and stripper column is lower for a lower solvent circulation. After the system has stabilized, the stripper sump level is constant which means that the water balance in the capture unit is stable. Regarding the integration of the capture unit and power plant, one can observe that the reboiler duty (Figure 5-2e) and the product gas flow (Figure 5-2f) show a smooth response.

The predicted transient responses for the increase in flue gas flow (case B) are as expected inverse but similar to case A (see Figure 5-3). However, the time necessary for the process variables to stabilize appears to be much shorter than in case A. This is the result of a larger solvent flow and a corresponding lower residence time. Again, the CO_2 product flow and the reboiler duty show a more gradual response than the perturbation. For the three cases the time for a few relevant variables to reach steady-state is compared (see Table 5-3). The time to reach steady-state is here defined as the minimum time after the perturbation required by the process variable to stay within a bandwidth of $\pm 1\%$ of its final value. As concluded with the figures, in case A the time to reach steady-state is significantly larger compared to cases B and C. For case A the time required to reach steady-state was three times higher than for cases B and C. The last dynamic case (see Figure 5-4) shows a response one would expect based on to the consecutive responses of case A and B. However, the values show smaller deviations than in cases A and B. This would again underline the conclusion that the capture unit shows a smooth response to a flue gas perturbation. Figures of other relevant variables can be found in Figures B-6 to B-8 in Appendix B.

Table 5-2: Steady-state process variable values for the three dynamic cases

		Baseline	Case A	Case B	Case C
Flue gas flow	[Nm^3/h]	1500	600	1500	1500
Lean solvent flow	[ton/h]	7.94	3.18	7.94	7.94
Capture rate	[%]	90.0	91.4	90.0	90.0
Rich loading	[mol/mol]	0.485	0.485	0.485	0.485
Lean loading	[mol/mol]	0.238	0.234	0.238	0.238
Reboiler pressure	[bar]	1.84	1.83	1.84	1.84
Product flow	[Nm^3/h]	188.2	76.3	188.2	188.2
Reboiler duty	[kW]	436.6	164.3	436.1	436.5
Specific heat duty	[kJ/kg]	4.33	4.01	4.32	4.33
Accumulated water	[kg]	0.0	0.9	-4.0	-0.9

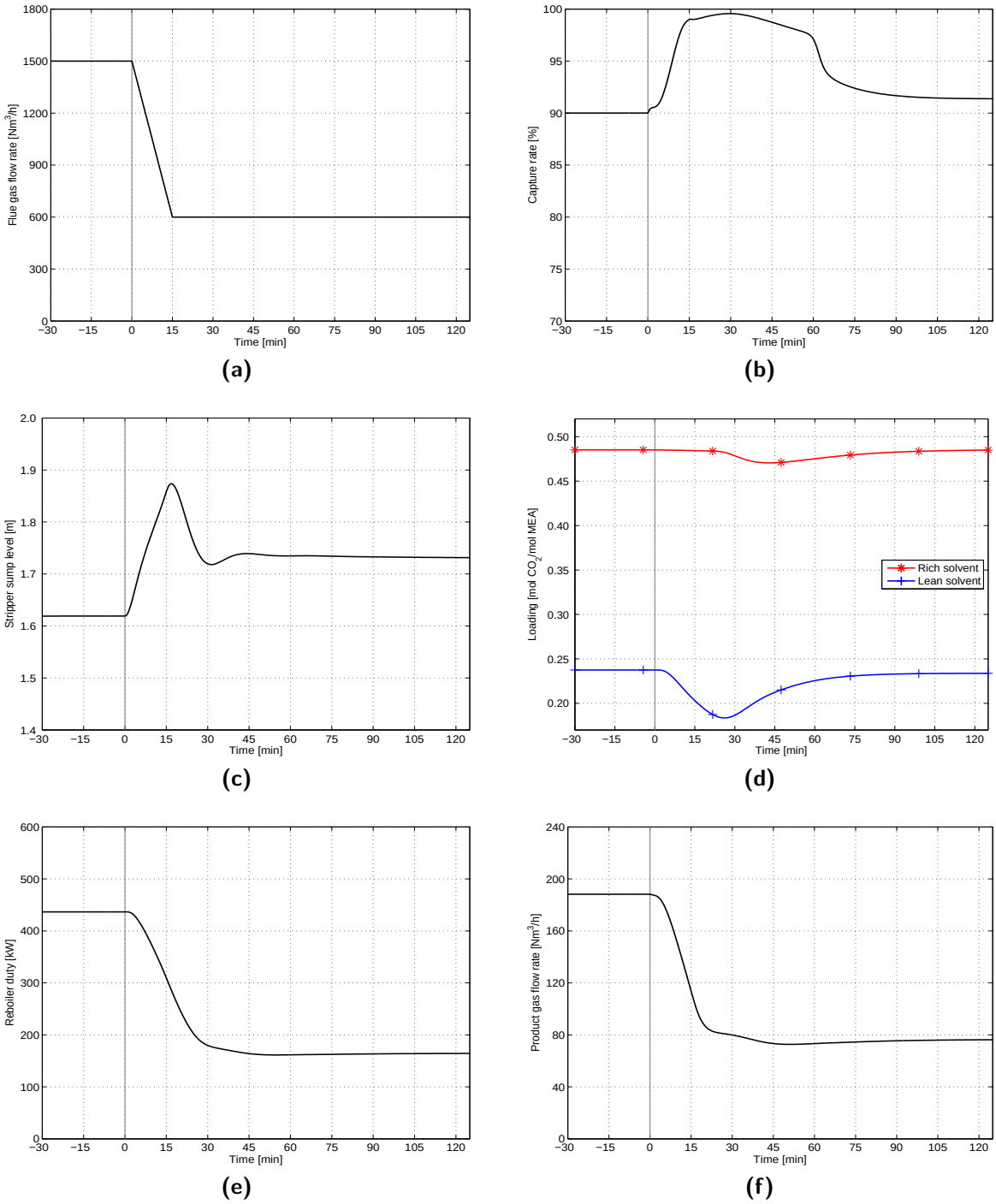

Figure 5-2: System response to a decrease of the flue gas flow rate (case A) of the flue gas flow rate (a), the capture rate (b), stripper sump level (c), rich and lean solvent loading (d), reboiler duty (e) and product gas flow (f)

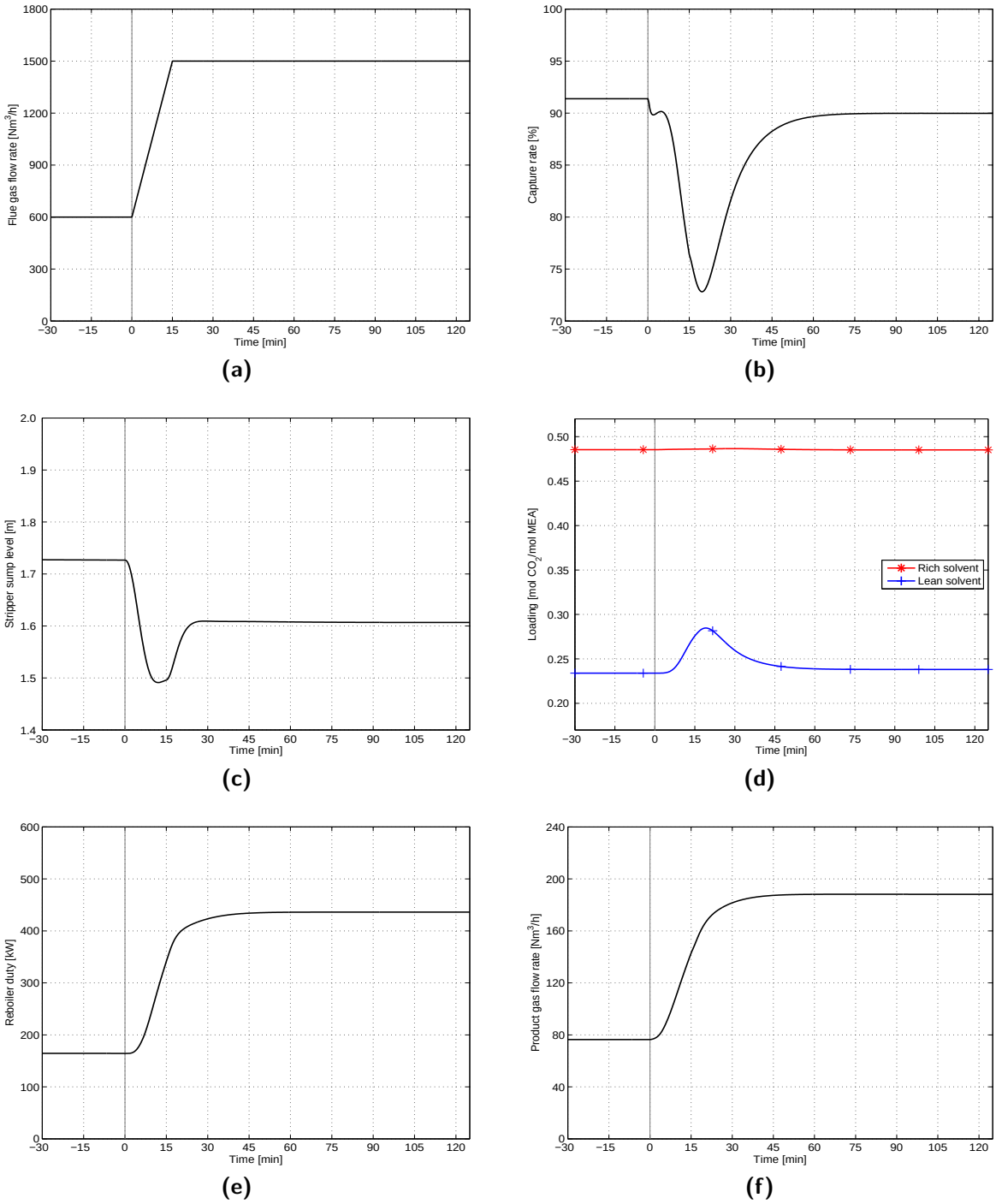

Figure 5-3: System response to an increase of the flue gas flow rate (case B) of the flue gas flow rate (a), the capture rate (b), stripper sump level (c), rich and lean solvent loading (d), reboiler duty (e) and product gas flow (f)

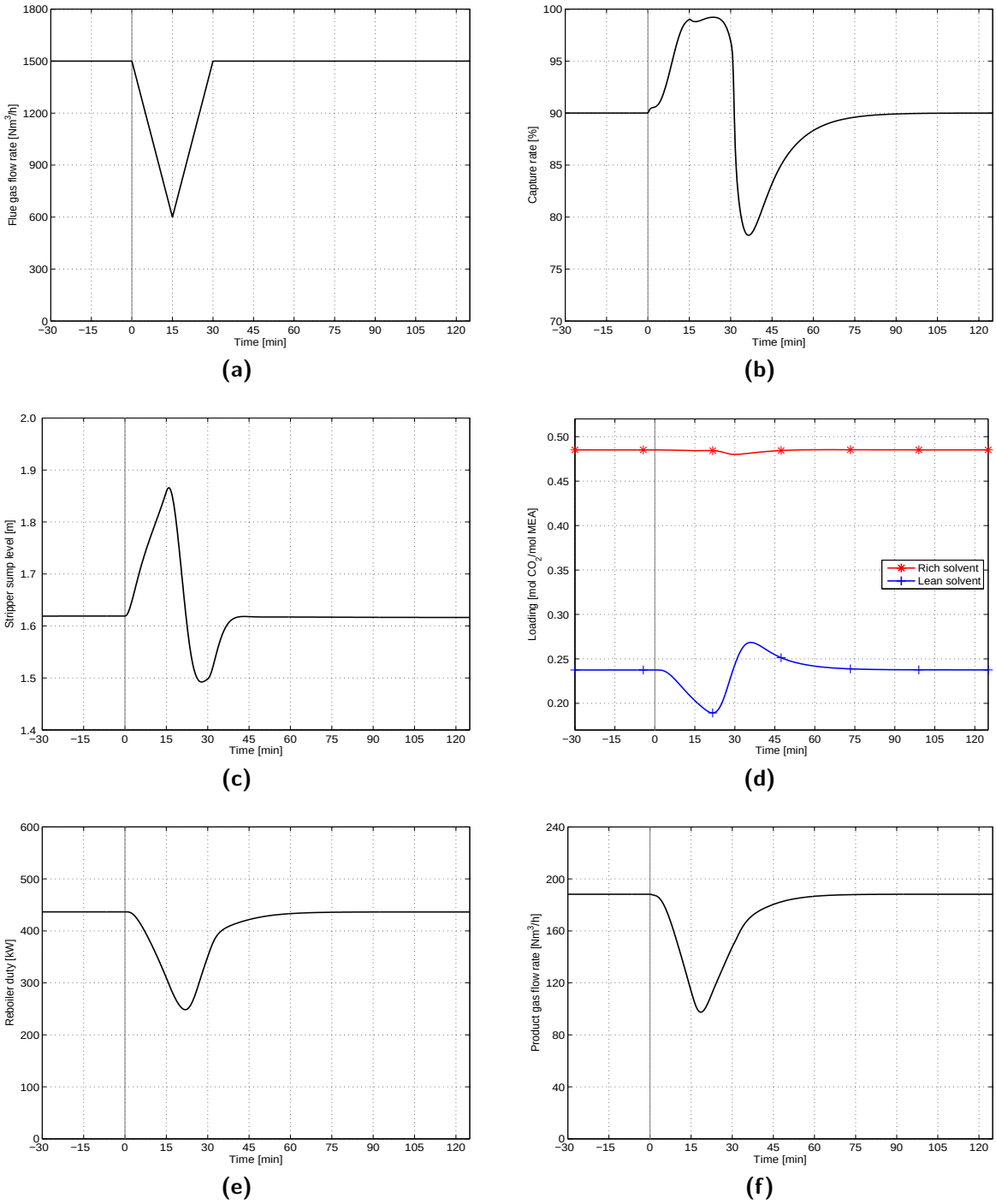

Figure 5-4: System response to a decrease and immediate increase of the flue gas flow rate (case C) of the flue gas flow rate (a), the capture rate (b), stripper sump level (c), rich and lean solvent loading (d), reboiler duty (e) and product gas flow (f)

Table 5-3: Elapsed time in minutes before steady-state of different process variables is reached for the dynamic test cases. The longest time per case is highlighted in bold.

	Case A	Case B	Case C
Rich loading	62	0	1
Lean Loading	63	**36**	36
Capture rate	61	**36**	**37**
Product flow	**78**	25	29
Reboiler duty	63	24	27

Chapter 6

Conclusion and recommendation

6-1 Conclusion

Based on the performed validation, it can be concluded that the simulated transient responses in terms of trend and time constant of the main process variables, such as capture rate, absorber temperature profile and solvent CO_2 loading are in good agreement with the experiments. Mismatches are observed for steady-state predictions of the absorber temperature profile and solvent CO_2 loading. However, to match steady-state results of the capture rate, the measurements of one of the main input variables, the flue gas flow rate, had to be corrected. The comparison of model predictions for the flue gas and solvent flow rate with the respective measurements revealed that the flow measurements are largely biased. In a future test campaign recalibration of the instruments is therefore recommended.
To assess the operational flexibility of a post-combustion capture unit integrated with a coal-fired power plant, three different operational scenarios were tested with the validated model. These test cases are based on a typical load following requirements for coal-fired power plants. To investigate the influence of the integration with the steam cycle of a coal-fired power plant and the compressor train, the reboiler duty and the CO_2 product flow rate are the variables of interest. Based on the simulation results, it can be concluded that the CO_2 product flow rate shows a smooth response to load variations of the power plant. Large flow fluctuations are not desirable for compressor train operation. It is observed that the response of the reboiler duty is very similar to the product flow rate. This is as well desirable as large fluctuations in the steam extraction at the steam turbines would have a large impact on the steam cycle in the power plant. In general, it can be concluded that the capture plant has a smooth response to a typical load variation of a power plant as no fast transients are observed in process variables which are integrated with other processes. From the case results it can also be observed that the required stabilization time of the capture plant is closely related the residence time related to the liquid hold-up in the system. For a larger solvent circulation flow, a lower residence time results in a significantly shorter stabilization time for the capture unit and vice versa. A control structure allowing load variations while maintaining a constant capture rate has been defined and implemented in the dynamic capture plant model. This control structure proofed to meet the requirements under the tested load variations.

6-2 Recommendation

In future research, more experiments to validate the dynamic model should be performed, especially the planned tests which were unsuccessful. Experiments with different step heights and simultaneous perturbation of both the solvent circulation flow and the flue gas flow are recommend. Secondly, to assess the performance of the commercial-scale capture unit the dynamic pilot plant model should be scaled up. Then the up-scaled model can be integrated with dynamic models of the coal-fired power plant, the compressor train and the pipeline and well system. To thoroughly investigate the interaction and constraints between the different processes during dynamic operation. With the integrated sytem model other operation modes, such as trip of the steam turbine or the capture plant and start-up an shut-down procedures could be investigated.
Regarding the dynamic models, the modeling of some components need to be improved to advance the performance predictability. The currently used model for the reboiler underpredicts the liquid hold-up. This has been resolved adjusting the geometrical size of the reboiler, but this limits the operation of the reboiler to its nominal condition. Additionally, discretizing the reboiler model would enable predicting of the temperature distribution in the reboiler in time during transient operation. This could point out possible hot spots in the reboiler which enhances solvent degradation. Including a model of the steam side of the reboiler with heat transfer correlations would give a more accurate prediction of the response time and enables integration with the steam cycle of the power plant.
The thermophysical media model used in this study is limited to a monoethanolamine (MEA) concentration of 7 mol MEA per kilogram of water. A solvent model which is capable to predict solubility properties for a wide range of solvent concentrations and also the availablity of different types of capture solvents would make the model more flexible and ease validation with data from other capture plants. A rate-based model for the chemical absorption process might improve the steady-state predictions in comparison to the equilibrium-based model currently used, but also increases computational time which is not beneficial, especially not considering the integration with dynamic models of the power plant.
In the current heat exchanger model, the heat transfer coefficient is assumed constant. In order to improve the accuracy of the heat exchanger performance predictions especially for operation whereby the flow rates are changing mass flow dependent heat transfer coefficients should be implemented and validated. This also improves the prediction of the specific heat duty per kilogram of carbon dioxide (CO_2). This which would make the model suitable for dynamic optimization in which the specific heat demand is minimized the energy consumption and costs.

Appendix A

Documentation of the component models

A-1 Packed column

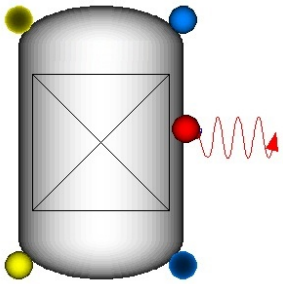

Figure A-1: Icon of random packed column model from the ThermalSeparation library

Component description

The packed column model describes the heat and mass transfer which takes place in a packed column. A separate gas and liquid phase are modelled. Correlations for mass transfer, medium properties, hold up and frictional loss are provided by other models. It is a module from the ThermalSeparation library.

Relevant phenomena

- Accumulation of mass and thermal energy in the gas and liquid phase
- Accumulation of thermal energy in the column packing
- Hold up of liquid in the column
- Mass transfer between gas and liquid
- Release of heat due to the absorption reaction
- Frictional losses on the gas side in the column

Hypothesis and assumptions

- Heat transfer to the packing material is very fast and therefore the packing temperature is equal to the liquid temperature
- Heat loss to the surrounding is negligible
- The absorption process in the packed column can be represented by a finite number of stages
- The heat capacity of the column packing material is constant.

Sub models

A heat sink is required to model heat loss to the environment. Inside the random packed column model the model for an adiabatic column can be selected. Also models for the media,

Model equations

Molar component balance for vapour phase

$$\frac{\mathrm{d}N_{\mathrm{i}}^{\mathrm{vap}}}{\mathrm{d}t} = \dot{N}_{\mathrm{in,i}}^{\mathrm{vap}} - \dot{N}_{\mathrm{out,i}}^{\mathrm{vap}} + \dot{N}_{\mathrm{trans,i}}^{\mathrm{vap}} \tag{A-1}$$

This equation can be rewritten for every stage j

$$\frac{A \cdot H \cdot \epsilon}{n} \cdot \frac{\mathrm{d}(\epsilon_{\mathrm{j}}^{\mathrm{vap}} \cdot c_{\mathrm{j,i}}^{\mathrm{vap}})}{\mathrm{d}t} = \dot{V}_{\mathrm{j-1}}^{\mathrm{vap}} c_{\mathrm{j-1,i}}^{\mathrm{vap}} - \dot{V}_{\mathrm{j}}^{\mathrm{vap}} c_{\mathrm{j,i}}^{\mathrm{vap}} + \dot{N}_{\mathrm{trans,j,i}}^{\mathrm{vap}} \tag{A-2}$$

Then, similar to equation A-1 a molar component balance for every component i in the liquid phase can be derived

$$\frac{\mathrm{d}N_{\mathrm{i}}^{\mathrm{liq}}}{\mathrm{d}t} = \dot{N}_{\mathrm{in,i}}^{\mathrm{liq}} - \dot{N}_{\mathrm{out,i}}^{\mathrm{liq}} + \dot{N}_{\mathrm{trans,i}}^{\mathrm{liq}} \tag{A-3}$$

This equation can as well be rewritten for every stage j

$$\frac{A \cdot H \cdot \epsilon}{n} \cdot \frac{\mathrm{d}(\epsilon_{\mathrm{j}}^{\mathrm{liq}} \cdot c_{\mathrm{j,i}}^{\mathrm{liq}})}{\mathrm{d}t} = \dot{V}_{\mathrm{j+1}}^{\mathrm{liq}} c_{\mathrm{j+1,i}}^{\mathrm{liq}} - \dot{V}_{\mathrm{j}}^{\mathrm{liq}} c_{\mathrm{j,i}}^{\mathrm{liq}} + \dot{N}_{\mathrm{trans,j,i}}^{\mathrm{liq}} \tag{A-4}$$

Total mole balance for the vapour phase

$$\frac{A \cdot H \cdot \epsilon}{n} \cdot \frac{\mathrm{d}(\epsilon_{\mathrm{j}}^{\mathrm{vap}} \cdot \rho_{\mathrm{j}}^{\mathrm{vap}} / MM^{\mathrm{vap}})}{\mathrm{d}t} = \dot{V}_{\mathrm{j-1}}^{\mathrm{vap}} \rho_{\mathrm{j-1}}^{\mathrm{vap}} / MM^{\mathrm{vap}} - \dot{V}_{\mathrm{j}}^{\mathrm{vap}} \rho_{\mathrm{j}}^{\mathrm{vap}} / MM^{\mathrm{vap}} + \sum \dot{N}_{\mathrm{trans,j}}^{\mathrm{vap}} \tag{A-5}$$

Total mole balance for the liquid phase

$$\frac{A \cdot H \cdot \epsilon}{n} \cdot \frac{\mathrm{d}(\epsilon_{\mathrm{j}}^{\mathrm{liq}} \cdot \rho_{\mathrm{j}}^{\mathrm{liq}} / MM^{\mathrm{liq}})}{\mathrm{d}t} = \dot{V}_{\mathrm{j-1}}^{\mathrm{liq}} \rho_{\mathrm{j-1}}^{\mathrm{liq}} / MM^{\mathrm{liq}} - \dot{V}_{\mathrm{j}}^{\mathrm{liq}} \rho_{\mathrm{j}}^{\mathrm{liq}} / MM^{\mathrm{liq}} + \sum \dot{N}_{\mathrm{trans,j}}^{\mathrm{liq}} \tag{A-6}$$

Energy balance for the liquid and packing material

$$\frac{A \cdot H \cdot \epsilon}{n} \cdot \frac{\mathrm{d}(\epsilon_{\mathrm{j}}^{\mathrm{liq}} \cdot \sum(c_{\mathrm{j,i}}^{\mathrm{liq}}) \cdot u^{\mathrm{liq}})}{\mathrm{d}t} + \frac{A \cdot H \cdot 1 - \epsilon}{n} \cdot \rho_{\mathrm{s}} \cdot c_{\mathrm{s}} \frac{\mathrm{d}T}{\mathrm{d}t}$$

$$= \dot{V}^{\text{liq}}_{\text{j+1}} \sum(c^{\text{liq}}_{\text{j+1}}) h^{\text{liq}}_{\text{j+1}} - \dot{V}^{\text{liq}}_{\text{j}} \sum(c^{\text{liq}}_{\text{j}}) h^{\text{liq}} + \dot{N}^{\text{liq}}_{\text{trans,j,i}} - \dot{Q}_{\text{wall}} + \dot{E}^{\text{liq}}_{\text{trans,j}} + \dot{Q}_{\text{reac}} \tag{A-7}$$

Energy balance for the vapour phase

$$\frac{A \cdot H \cdot \epsilon}{n} \cdot \frac{\text{d}(\epsilon^{\text{vap}}_{\text{j}} \cdot \sum(c^{\text{vap}}_{\text{j,i}}) \cdot u^{\text{vap}})}{\text{d}t}$$

$$= \dot{V}^{\text{vap}}_{\text{j-1}} \sum(c^{\text{vap}}_{\text{j-1}}) h^{\text{vap}}_{\text{j-1}} - \dot{V}^{\text{vap}}_{\text{j}} \sum(c^{\text{vap}}_{\text{j}}) h^{\text{vap}}_{\text{j}} + \dot{N}^{\text{liq}}_{\text{trans,j,i}} + \dot{E}^{\text{vap}}_{\text{trans,j}} \tag{A-8}$$

Model input and output variables and parameters

The packed column model accounts for storage and resistive phenomena in the gas and liquid phase on each stage and is therefore on both sides a S-R type of module. In accordance with the causality, (molar) gas and liquid flow and specific molar enthalpy should be specified at the inlet, while the pressure should be specified at the outlet gas and liquid stream of the model. In the system model this values are given as inputs by up and downstream models. The geometry depends on the real column packing geometry and should be defined with a height, diameter, void fraction and relative surface area of the packing.

Table A-1: Model input and output variables and parameters for the packed column module

Input variables	$P^{\text{vap}}_{\text{out}}$, $P^{\text{liq}}_{\text{out}}$, $\dot{N}^{\text{vap}}_{\text{in}}$, $\dot{N}^{\text{liq}}_{\text{in}}$, $x^{\text{vap}}_{\text{in}}$, $x^{\text{liq}}_{\text{in}}$, $h^{\text{vap}}_{\text{in}}$, $h^{\text{liq}}_{\text{in}}$
Output variables	$P^{\text{vap}}_{\text{in}}$, $P^{\text{liq}}_{\text{in}}$, $\dot{N}^{\text{vap}}_{\text{out}}$, $\dot{N}^{\text{liq}}_{\text{out}}$, $x^{\text{vap}}_{\text{out}}$, $x^{\text{liq}}_{\text{out}}$, $h^{\text{vap}}_{\text{out}}$, $h^{\text{liq}}_{\text{out}}$
Parameters	A, H, ε, n

A-2 Reboiler

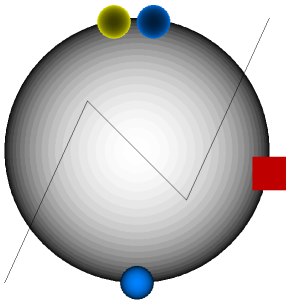

Figure A-2: Icon of reboiler model from the ThermalSeparation library

Component description

The reboiler model is a single stage equilibrium model, comparable to a stage in the random packed column model. It has a heat input to boil up the liquid. The outlet is two phase; therefore there is only a liquid inlet and a liquid and vapour outlet.

Relevant phenomena

- Heat input from a heat source to the fluid
- Heat and mass transfer between the liquid and vapour phase
- Evaporation of liquid
- Hydrostatic pressure build up in the reboiler in the liquid

Hypothesis and assumptions

- Vapour and liquid is in thermal and chemical equilibrium
- The heat from the heat source is transferred to the liquid side
- Hydrostatic conditions (negligible fluid velocities)
- The liquid/vapour mixture is ideally mixed, the outlet composition and temperature are equal to the one in the reboiler

Model equations

Molar component balance for vapour phase

$$\frac{\mathrm{d}N_{\mathrm{i}}^{\mathrm{vap}}}{\mathrm{d}t} = \dot{N}_{\mathrm{in,i}}^{\mathrm{vap}} - \dot{N}_{\mathrm{out,i}}^{\mathrm{vap}} + \dot{N}_{\mathrm{trans,i}}^{\mathrm{vap}} \tag{A-9}$$

Molar component balance for liquid phase

$$\frac{\mathrm{d}N_{\mathrm{i}}^{\mathrm{liq}}}{\mathrm{d}t} = \dot{N}_{\mathrm{in,i}}^{\mathrm{liq}} - \dot{N}_{\mathrm{out,i}}^{\mathrm{liq}} + \dot{N}_{\mathrm{trans,i}}^{\mathrm{liq}} \tag{A-10}$$

Total mole balance vapour

$$\frac{\mathrm{d}N^{\mathrm{vap}}}{\mathrm{d}t} = V \cdot \frac{\mathrm{d}\left(\epsilon^{\mathrm{vap}} \cdot \rho^{\mathrm{vap}}/MM^{\mathrm{vap}}\right)}{\mathrm{d}t} = \dot{N}_{\mathrm{in}}^{\mathrm{vap}} - \dot{N}_{\mathrm{out}}^{\mathrm{vap}} + \sum \dot{N}_{\mathrm{transfer}}^{\mathrm{vap}} \tag{A-11}$$

Total mole balance liquid

$$\frac{\mathrm{d}N^{\mathrm{liq}}}{\mathrm{d}t} = V \cdot \frac{\mathrm{d}\left(\epsilon^{\mathrm{liq}} \cdot \rho^{\mathrm{liq}}/MM^{\mathrm{liq}}\right)}{\mathrm{d}t} = \dot{N}_{\mathrm{in}}^{\mathrm{liq}} - \dot{N}_{\mathrm{out}}^{\mathrm{liq}} + \sum \dot{N}_{\mathrm{transfer}}^{\mathrm{liq}} \tag{A-12}$$

Energy balance for the liquid

$$\frac{\mathrm{d}U}{\mathrm{d}t} = V \cdot \frac{\mathrm{d}\left(\epsilon^{\mathrm{liq}} \sum c^{\mathrm{liq}} \cdot u^{\mathrm{liq}}\right)}{\mathrm{d}t} = \dot{N}_{\mathrm{in}}^{\mathrm{liq}} \cdot h_{\mathrm{in}}^{\mathrm{liq}} - \dot{N}_{\mathrm{out}}^{\mathrm{liq}} \cdot h_{\mathrm{out}}^{\mathrm{liq}} + \dot{E}_{\mathrm{transfer}}^{\mathrm{liq}} + \Delta H_r + \dot{Q}_{wall} \tag{A-13}$$

Energy balance for the vapour

$$\frac{\mathrm{d}U}{\mathrm{d}t} = V \cdot \frac{\mathrm{d}\left(\epsilon^{\mathrm{vap}} \sum c^{\mathrm{vap}} \cdot u^{\mathrm{vap}}\right)}{\mathrm{d}t} = \dot{N}_{\mathrm{in}}^{\mathrm{vap}} \cdot h_{\mathrm{in}}^{\mathrm{vap}} - \dot{N}_{\mathrm{out}}^{\mathrm{liq}} \cdot h_{\mathrm{out}}^{\mathrm{vap}} + \dot{E}_{\mathrm{transfer}}^{\mathrm{vap}} \tag{A-14}$$

Model equations in the equilibrium approach.

$$\dot{N}_i^{\mathrm{vap}} = \dot{Z}_i^{\mathrm{vap}} \cdot (y_i - y_i^*) \tag{A-15}$$

$$\dot{N}_i^{\text{liq}} = \dot{Z}_i^{\text{liq}} \cdot (x_i - x_i^*) \tag{A-16}$$

Where Z is an adjustable factor. For the inert components:

$$\dot{N}_i = 0 \tag{A-17}$$

$$\dot{Q}^{\text{vap}} = Z \cdot (T^* - T^{\text{vap}}) \tag{A-18}$$

$$\dot{Q}^{\text{liq}} = Z \cdot (T^* - T^{\text{liq}}) \tag{A-19}$$

Where Z is again an adjustable factor.

The hydrostatic pressure drop is dependent on the liquid content

$$P_{\text{out}}^{\text{liq}} - P_{\text{in}}^{\text{liq}} = length_{\text{HX}} \cdot \epsilon^{\text{liq}} \cdot \rho^{\text{liq}} \cdot g \tag{A-20}$$

As it is assumed that the outlet conditions are equal to the one in the reboiler, the vapour and liquid flow are coupled:

$$\dot{V}^{\text{liq}} = \dot{V}^{\text{vap}} \cdot \frac{\epsilon^{\text{liq}}}{\epsilon^{\text{vap}}} \tag{A-21}$$

Model input and output variables and parameters

On the liquid side the reboiler module is a S-R type of module, and on the vapour side a R type of module. Therefore the inlet mass flow and outlet pressure is an input and the outlet massflow and inlet pressure an output variable (see Table A-2).

Table A-2: Model input and output variables and parameters for the reboiler module

Input variables	$P_{\text{out}}^{\text{vap}}$, $P_{\text{out}}^{\text{liq}}$, $\dot{N}_{\text{in}}^{\text{liq}}$, $x_{\text{in}}^{\text{liq}}$, $h_{\text{in}}^{\text{liq}}$, $\dot{Q}_{\text{wall}}$
Output variables	$P_{\text{in}}^{\text{liq}}$, $\dot{N}_{\text{out}}^{\text{vap}}$, $\dot{N}_{\text{out}}^{\text{liq}}$, $x_{\text{out}}^{\text{vap}}$, $x_{\text{out}}^{\text{liq}}$, $h_{\text{out}}^{\text{vap}}$, $h_{\text{out}}^{\text{liq}}$
Parameters	dtube, dHX, $length_{\text{HX}}$, n

A-3 Valve

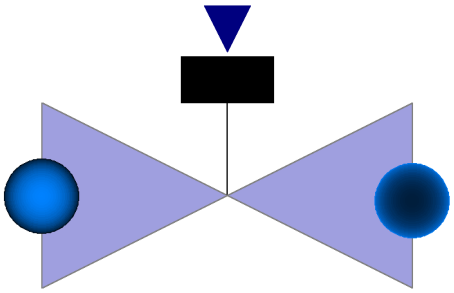

Figure A-3: Adapted valve icon from the ThermoPower library

Component description

In the valve component the mass flow is calculated with a provided pressure drop and valve opening. For the relation between valve opening and flow coefficient K_v there can be chosen for a linear, quadratic or equal percentage. The valve component is taken from the ThermoPower library and its connectors and equations are adapted to molar flows and composition in order to be consistent with the models taken from ThermalSeparation.

Relevant phenomena

- Flow dependent on valve opening and pressure drop over the valve

Hypothesis and assumptions

- No accumulation of mass, energy and momentum
- No shaft work or heat transfer
- Flow can be approximated as a flow through a circular pipe
- Full turbulent 1D flow
- The flow is incompressible
- No reactions take place

Model equations

Conservation equations

Mass conservation, no accumulation of mass

$$\frac{\mathrm{d}M}{\mathrm{d}t} = \dot{m}_{\mathrm{in}} - \dot{m}_{\mathrm{out}} = 0 \tag{A-22}$$

No reactions take place, thus we can rewrite the equation in molar form

$$\dot{N}_{\mathrm{in}} = \dot{N}_{\mathrm{out}} \tag{A-23}$$

Energy conservation

$$\frac{\mathrm{d}U}{\mathrm{d}t} = \dot{m}_{\mathrm{in}} \cdot h_{\mathrm{in}} - \dot{m}_{\mathrm{out}} \cdot h_{\mathrm{out}} + \dot{Q} - W_{\mathrm{S}} - P\frac{\mathrm{d}V}{\mathrm{d}t} \tag{A-24}$$

is reduced to

$$0 = \dot{m}_{\mathrm{in}} \cdot h_{\mathrm{in}} - \dot{m}_{\mathrm{out}} \cdot h_{\mathrm{out}} \tag{A-25}$$

Combined with equation A-22 this leads to

$$h_{\mathrm{in}} = h_{\mathrm{out}} \tag{A-26}$$

Conservation of momentum

$$\frac{\mathrm{d}G}{\mathrm{d}t} = \dot{m}_{\mathrm{in}} \cdot v_{\mathrm{in}} - \dot{m}_{\mathrm{out}} \cdot v_{\mathrm{out}} + (S_{in} \cdot P_{in} - S_{\mathrm{out}} \cdot P_{\mathrm{out}} - F_{\mathrm{ff}}) + S \cdot \rho g \cdot (z_{\mathrm{in}} - z_{\mathrm{out}}) \tag{A-27}$$

No accumulation of momentum, change in kinetic and potential energy can be neglected, constant cross section, therefore:

$$S(P_{in} - P_{\text{out}}) = F_{\text{ff}} \tag{A-28}$$

Constitutive equations
Darcy-Weisbach law for energy loss due friction

$$\xi = \Psi \cdot \frac{L}{D} \cdot \frac{v^2}{2g} \tag{A-29}$$

where

$$\Psi = f(Re, \frac{e}{d}) \tag{A-30}$$

$$\xi = C \cdot \frac{v^2}{2g} \tag{A-31}$$

Energy loss can be converted to pressure drop via:

$$\Delta P = \rho g \xi \tag{A-32}$$

Friction force

$$F_{\text{ff}} = S\Delta P = S\rho g(C \cdot \frac{v^2}{2g}) \tag{A-33}$$

Velocity

$$v = \frac{\dot{m}}{\rho S} \tag{A-34}$$

$$\Delta P = S\rho g \left(C \cdot \frac{(\frac{\dot{m}}{\rho S})^2}{2g} \right) = \frac{C f^2}{2\rho S^2} \rightarrow \dot{m} = \sqrt{\frac{2\rho S^2}{C} \Delta P} \tag{A-35}$$

Since S is a constant, we can introduce a flow coefficient K_v

$$\dot{m} = K_v \sqrt{\rho \Delta P} \tag{A-36}$$

Introducing valve opening

$$\dot{m} = f(\theta) K_v \sqrt{\rho \Delta P} \tag{A-37}$$

Where $f(\theta)$ is a function of the valve opening θ, which can be assumed linear, quadratic or equal percentage depending on the valve type.

Table A-3: Model input and output variables and parameters for the valve module

Input variables	P_{in}, P_{out}, h_{in}, x_{in}, ρ
Output variables	$\dot{N}_{\text{in}}$, $\dot{N}_{\text{out}}$, h_{out}, x_{out}
Parameter	K_v

A-4 Heat exchanger

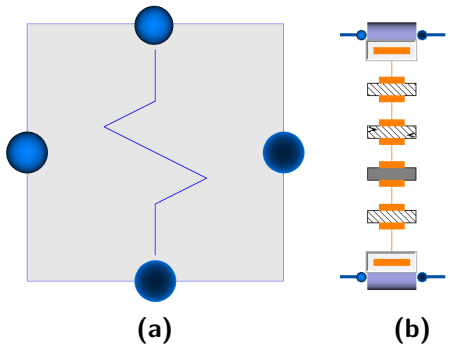

Figure A-4: Icon for the heat exchanger model (a) and its model structure (b)

Component description

In the heat exchanger model, thermal energy is exchanged between two fluids. A wall separates the two fluid control volumes from each other. The heat transfer is dependent on the temperature difference between the fluid and the metal wall. Pressure drop can be accounted for on both fluid sides. The heat exchanger model for gases has taken from the ThermoPower library. This model accounts for the mixture composition. Its connectors and equations are adapted to molar flows and composition in order to be consistent with the models taken from ThermalSeparation.

Relevant phenomena

- Heat transfer from hot fluid to cold fluid
- Frictional losses in both flows
- Accumulation of mass and thermal energy in both fluid flows
- Accumulation of thermal energy in the metal wall

Hypothesis and assumptions

- No shaft work
- Change in kinetic and potential energy is negligible
- Heat transfer is convective
- No accumulation of energy in heat exchanger casing
- Single phase flow on both sides
- Uniform velocity on cross section (1D flow)
- Flow is incompressible (for liquid)
- No reactions take place
- Uniform composition of the fluid along heat exchanger length (ideally mixed)

Sub models

The heat exchanger component is divided into two fluid control volumes and a wall control volume. Both fluid flows consist of a fluid resistive (if pressure drop is taken into account) and a fluid storage sub module. The metal wall consist of a thermal storage module, and on both sides a thermal resistive module for heat transfer.

Model equations

Fluid control volume
Conservation of mass

$$\frac{\mathrm{d}M}{\mathrm{d}t} = \frac{\mathrm{d}(\bar{\rho}V)}{\mathrm{d}t} = V \cdot \frac{\mathrm{d}\bar{\rho}}{\mathrm{d}t} = A \cdot l \left(\frac{\partial \rho}{\partial p} \cdot \frac{\mathrm{d}p}{\mathrm{d}t} + \frac{\partial \rho}{\partial T} \cdot \frac{\mathrm{d}T}{\mathrm{d}t} + \frac{\partial \rho}{\partial x_\mathrm{i}} \cdot \frac{\mathrm{d}x_\mathrm{i}}{\mathrm{d}t} \right) \tag{A-38}$$

The flow is assumed to be incompressible and change in composition with respect to time is small, thus:

$$\frac{\mathrm{d}M}{\mathrm{d}t} = \dot{M}_\mathrm{in} - \dot{M}_\mathrm{out} = A \cdot l \left(\frac{\partial \rho}{\partial T} \cdot \frac{\mathrm{d}T}{\mathrm{d}t} \right) \tag{A-39}$$

Component balance

$$\frac{\mathrm{d}N_\mathrm{i}}{\mathrm{d}t} = \frac{\mathrm{d}x_\mathrm{i}N_\mathrm{tot}}{\mathrm{d}t} = \dot{N}_\mathrm{in,i} - \dot{N}_\mathrm{out,in} = x_\mathrm{in,i}\dot{N}_\mathrm{in} - x_\mathrm{out,i}\dot{N}_\mathrm{out} \tag{A-40}$$

$$\frac{\mathrm{d}x_\mathrm{i}}{\mathrm{d}t} = \frac{x_\mathrm{in,i}\dot{N}_\mathrm{in} - x_\mathrm{out,i}\dot{N}_\mathrm{out}}{N_\mathrm{tot}} = \frac{x_\mathrm{in,i}\dot{N}_\mathrm{in} - x_\mathrm{out,i}\dot{N}_\mathrm{out}}{A \cdot l \cdot \bar{\rho}/MM} \tag{A-41}$$

Conservation of momentum

$$\frac{\mathrm{d}G}{\mathrm{d}t} = \frac{\mathrm{d}(\bar{\rho}V\bar{v})}{\mathrm{d}t} = f_\mathrm{E}v_\mathrm{E} - f_\mathrm{L}v_\mathrm{L} + S_\mathrm{E}P_\mathrm{E} - S_\mathrm{L}P_\mathrm{L} - F_\mathrm{W} + S\rho g(z_\mathrm{E} - z_\mathrm{L}) \tag{A-42}$$

No accumulation of momentum, change in kinetic and potential energy can be neglected, constant cross section, therefore:

$$P_{in} - P_\mathrm{out} = \frac{F_\mathrm{ff}}{S} = \Delta P_\mathrm{fric} \tag{A-43}$$

Conservation of energy

$$\frac{\mathrm{d}U}{\mathrm{d}t} = \frac{\mathrm{d}(V \cdot \bar{\rho} \cdot \bar{c}_\mathrm{p} \cdot T)}{\mathrm{d}t} = \bar{\dot{m}}(h_\mathrm{in} - h_\mathrm{out}) + \dot{Q} \tag{A-44}$$

$$\dot{Q} = l \cdot \Omega \cdot \bar{\dot{\phi}} \tag{A-45}$$

$$V \cdot \bar{\rho} \cdot \bar{c}_\mathrm{p} \cdot \frac{\mathrm{d}T}{\mathrm{d}t} = \bar{\dot{m}}(h_\mathrm{in} - h_\mathrm{out}) + l \cdot \Omega \cdot \bar{\dot{\phi}} \tag{A-46}$$

Thermal resistive module
The heat flow is calculated with the temperature difference

$$Q = \Gamma \cdot A \cdot \Delta T \tag{A-47}$$

Γ is the heat transfer coefficient of the fluid to the wall

$$\phi = \frac{Q}{A} = \Gamma \cdot \Delta T \tag{A-48}$$

Thermal storage module
The energy balance can be written as:

$$\frac{\mathrm{d}U}{\mathrm{d}t} = \frac{\mathrm{d}(M \cdot c_{\mathrm{m}} T)}{\mathrm{d}t} = M \cdot c_{\mathrm{m}} \cdot \frac{\mathrm{d}T}{\mathrm{d}t} = S_{\mathrm{int}} \cdot \dot{\phi}_{\mathrm{int}} - S_{\mathrm{ext}} \cdot \dot{\phi}_{\mathrm{ext}} \tag{A-49}$$

Model input and output variables and parameters

If pressure loss due to friction is taken into account, the module is on the fluid side R-S or S-R depending on the location where the pressure drop is lumped. If pressure loss is neglected, the component is purely a storage module. This choice depends on the causality of the combined system. At the resistive side, pressure is an input variable and flow an output variable. At the storage side this is reversed and flow is the input variable and pressure the output variable.

A-5 Sump

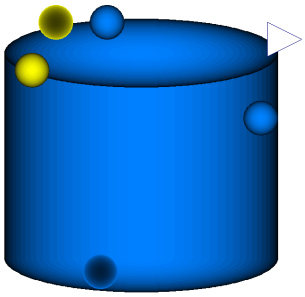

Figure A-5: Icon of the sump model from the ThermalSeparation library

Component description

In the sump, liquid is collected to act as a buffer to downstream processes and prevent cavitation in pumps. The sump module is a module from the Thermal Separation library. It has a liquid in and outlet and a vapour in and outlet which is required to calculate the outlet pressure.

Relevant phenomena

- Accumulation of mass and energy in the liquid phase

Hypothesis and assumptions

- The thermal conductivity of the liquid is high and the liquid is well-mixed (homogeneous composition and temperature)
- Heat transfer to the surroundings is negligible
- Hydrostatic conditions (negligible fluid velocities)
- Liquid is incompressible
- No reactions take place
- No heat and mass transfer between the vapour and liquid phase

Sub models

Only the liquid and vapour media model should be selected. As stated earlier, the vapour medium is only used to calculate liquid outlet pressure, the input vapour variables at the inlet are directed to the outlet and vice versa.

Model equations

Mole balance for every component in the liquid phase without reactions taking place

$$\frac{\mathrm{d}N_{\mathrm{i}}}{\mathrm{d}t} = \dot{N}_{\mathrm{in,i}} - \dot{N}_{\mathrm{out,i}} \tag{A-50}$$

$$A{\cdot}\mathrm{MM}_{\mathrm{l,i}}{\cdot}\frac{\mathrm{d}(\mathrm{level}{\cdot}\rho_{\mathrm{l}}{\cdot}x_{\mathrm{l,i}}/\mathrm{MM}_{\mathrm{l,tot}})}{\mathrm{d}t} = \dot{N}_{\mathrm{in}}{\cdot}x_{\mathrm{l,in,i}}{\cdot}\mathrm{MM}_{\mathrm{l,i}} + \dot{N}_{\mathrm{out}}{\cdot}x_{\mathrm{l,out,i}}{\cdot}\mathrm{MM}_{\mathrm{l,i}} \tag{A-51}$$

Energy balance

$$\frac{\mathrm{d}U}{\mathrm{d}t} = \dot{m}_{\mathrm{in}}{\cdot}h_{\mathrm{in}} - \dot{m}_{\mathrm{out}}{\cdot}h_{\mathrm{out}} + \dot{Q} - W_{\mathrm{S}} - P\frac{\mathrm{d}V}{\mathrm{d}t} \tag{A-52}$$

No work, heat transfer, moving boundaries and rewritten to molar form

$$\frac{\mathrm{d}U}{\mathrm{d}t} = A{\cdot}\frac{\mathrm{d}(c_{\mathrm{l,tot}}{\cdot}u_{\mathrm{l}}{\cdot}\mathrm{level})}{\mathrm{d}t} = \dot{N}_{\mathrm{in}}{\cdot}h_{\mathrm{in}} - \dot{N}_{\mathrm{out}}{\cdot}h_{\mathrm{out}} \tag{A-53}$$

Model input and output variables and parameters

Since the sump module is a storage module, inlet and outlet flows are an input variable and the inlet and outlet pressure are output variables.

Table A-4: Model input and output variables and parameters for the sump model

Input variables	$\dot{N}_{\mathrm{in}}$, $\dot{N}_{\mathrm{out}}$, h_{in}, x_{in}, P_{in}
Output variables	P_{out}, h_{out}, x_{out}, level
Parameters	dsump

A-6 Pump

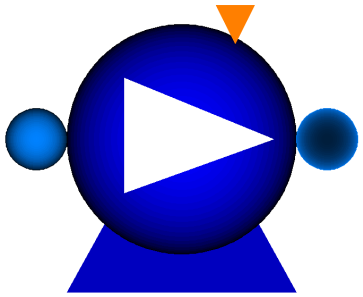

Figure A-6: Pump icon adapted from the Thermopower library

Component description

In the pump the pressure of the fluid increases. This module is adapted from the ThermoPower library. Connectors are adjusted to connect to the Thermal Separation components and equations are rewritten in molar form.

Relevant phenomena

- Work transferred by the pump to the fluid
- Pressure increase in the fluid

Hypothesis and assumptions

- The volume of the pump can be neglected (no accumulation of mass and energy)
- The pump runs at its nominal speed

Model equations

Conservation of mass

$$\frac{\mathrm{d}M}{\mathrm{d}t} = \dot{m}_{\mathrm{in}} - \dot{m}_{\mathrm{out}} = 0 \tag{A-54}$$

When there is no accumulation of mass, then

$$\dot{m}_{\mathrm{in}} = \dot{m}_{\mathrm{out}} \tag{A-55}$$

Since no reactions take place we can write this in molar form as

$$\dot{N}_{\mathrm{in}} = \dot{N}_{\mathrm{out}} \tag{A-56}$$

Conservation of energy

$$\frac{\mathrm{d}U}{\mathrm{d}t} = \dot{m}_{\mathrm{in}} \cdot h_{\mathrm{in}} - \dot{m}_{\mathrm{out}} \cdot h_{\mathrm{out}} + \dot{Q} - W_{\mathrm{S}} - P\frac{\mathrm{d}V}{\mathrm{d}t} \tag{A-57}$$

Heat loss can be neglected, no moving boundary and work is done on the system, thus

$$0 = \dot{m}_{\mathrm{in}} \cdot h_{\mathrm{in}} - \dot{m}_{\mathrm{out}} \cdot h_{\mathrm{out}} + W_{\mathrm{S}} \tag{A-58}$$

$$\Delta P = \rho g head \tag{A-59}$$

Nominal head is a function of nominal flow and is given by the manufacturer

$$head_{\text{nom}} = f(q_{\text{nom}}) \tag{A-60}$$

Power is as well a function of the flow and should be corrected for the actual density

$$W = f(q_{\text{nom}}) \cdot \frac{\rho}{\rho_{\text{nom}}} \tag{A-61}$$

This function is assumed to be quadratic and determined by three operating points of the pump specifications.

Then, the efficiency can be calculated

$$\eta = \frac{q \cdot \Delta P}{W} \tag{A-62}$$

Model input and output variables and parameters

The pump is a resistive module, which means that inlet and outlet pressure are an input and the flow is a resulting output variable(see TableA-5).

Table A-5: Model input and output variables for the pump module

Input variables	P_{in}, P_{out}, h_{in}, x_{in}
Output variables	$\dot{N}_{\text{in}}$, $\dot{N}_{\text{out}}$, h_{out}, x_{out}

A-7 H_2O-CO_2-MEA media model

Model description

A media model is required of the prediction of the absorption of carbon dioxide (CO_2) and related heat of absorption, and for the prediction of media properties as density and heat capacity. For this properties, validated empirical correlations are used.

Relevant phenomena

- Absorption of CO_2 by the solvent
- Release of heat due to exothermic absorption reaction
- Solvent properties dependent on conditions

Hypothesis and assumptions

- In the liquid only water, carbon dioxide and monoethanolamine are present[1]
- The reactions that take place are in equilibrium
- The liquid is in thermal equilibrium with the gas
- The solvent concentration is constant at 7 molality[2]

Model equations

J. Oexmann developed empirical correlations for the density, heat capacity and CO_2 solubility of the MEA solvent. The correlations are based on experimental results and presented in [36]. For the density the following correlation dependent on loading, temperature and the molality($\bar{m}_{alk}$) of the solvent has been developed:

$$\begin{aligned}\rho = {} & c_{dens,0} + c_{dens,1}\ t + c_{dens,2}\ t^2 + c_{dens,3}\ \alpha + c_{dens,4}\ \alpha^2 \\ & + c_{dens,5}\ \bar{m}_{alk} + c_{dens,6}\ \bar{m}_{alk}^2 + c_{dens,7}\ \alpha\ \bar{m}_{alk}\end{aligned} \tag{A-63}$$

For the heat capacity in a similar way the following empirical correlation has been developed:

$$\begin{aligned}C_{p,L} = {} & c_{Cp,0} + c_{Cp,1}\ t + c_{Cp,2}\ t^2 + c_{Cp,3}\ \alpha + c_{Cp,4}\ \alpha^2 + c_{Cp,5}\ \bar{m}_{alk} \\ & + c_{Cp,6}\ \bar{m}_{alk}^2 + c_{Cp,7}\ t\ \alpha + c_{Cp,8}\ t\ \bar{m}_{alk} + c_{Cp,9}\ \alpha\ \bar{m}_{alk} + c_{Cp,9}\ t\ \alpha\ \bar{m}_{alk}\end{aligned} \tag{A-64}$$

The CO_2 solubility is dependent on the loading and temperature of the solvent. It should be noted that the correlation only holds for a MEA-based solvent with a molality of 7 mol MEA/kg water.

$$\begin{aligned}\ln p^*_{CO2} = {} & c_{pco2,0} + c_{pco2,1}\ \frac{1}{T} + c_{pco2,2}\ \alpha + c_{pco2,3}\ \frac{\alpha}{T} + c_{pco2,4}\ \alpha^2 \\ & + c_{pco2,5}\ \frac{\alpha^2}{T} + c_{pco2,6}\ \alpha^3 + c_{pco2,7}\ \frac{\alpha^3}{T} + c_{pco2,8}\ \alpha^4\end{aligned} \tag{A-65}$$

The heat of absorption can then be calculated by using the Gibbs-Helmholtz equation

$$\frac{d(\ln p^*_{CO2})}{d(1/T)} = -\frac{\Delta h_{abs,CO_2}}{R} \tag{A-66}$$

by deriving equation A-65 with respect to 1/T and including the result in equation A-66 the following equation for the heat of absorption can be obtained

$$\Delta h_{abs,CO_2} = -R(c_{pco2,1} + c_{pco2,3}\ \alpha + c_{pco2,5}\ \alpha^2 + c_{pco2,7}\ \alpha^3) \tag{A-67}$$

[1] Although also carbamates are present in the solvent, by use of empirical correlations for CO_2 solubility and solvent properties in the H_2O-CO_2-MEA media model, modeling of other components is not relevant.

[2] The molality is defined as the amount of substance in mol divided by the mass of the solute (here water). Unlike molarity, this is independent of the presence of other components in the solvent. A molality for MEA in water of 7 corresponds with a 30 weight percent solution of (unloaded) MEA.

Table A-6: Model input and output variables for the H_2O-CO_2-MEA media model

Input variables	P, T, x_i
Output variables	ρ, C_p, h, $\Delta h_{\mathrm{abs,CO_2}}$, p^*_{CO2}

Table A-7: Coefficients to determine density via Eq. A-63 [36]

$\bar{m}_\mathrm{alk}$	1.8-10.9 m
range	
t	25-80 °C
α	0-0.5
$c_{\mathrm{dens},0}$	1.005E+03
$c_{\mathrm{dens},1}$	−5.993E−01
$c_{\mathrm{dens},2}$	0
$c_{\mathrm{dens},3}$	2.492E+01
$c_{\mathrm{dens},4}$	1.135E+02
$c_{\mathrm{dens},5}$	6.172E+00
$c_{\mathrm{dens},6}$	−3.570E−01
$c_{\mathrm{dens},8}$	1.917E+01
n^*	127
$\sigma^\dagger$	0.30 %

$^*n$ is the number of data points

$^\dagger\sigma = \frac{1}{n}\sum_1^n \left(\frac{|\rho_{\mathrm{p,exp}}-\rho_{\mathrm{p,calc}}|}{\rho_{\mathrm{p,exp}}}\right)$

A-8 Stichlmair pressure loss correlation

Component description

The Stichlmair pressure drop correlation is used to calculate the frictional loss in the column. The model equations are derived from the model presented in Ref. [37].

Relevant phenomena

- Resistive pressure drop on the gas side

Hypothesis and assumptions

- In every stage the pressure drop is constant per unit of length

Model equations

Reynolds number of the gas

$$Re_\mathrm{g} = \frac{d_\mathrm{p} U_\mathrm{g} \rho_\mathrm{g}}{\mu} \tag{A-68}$$

Table A-8: Coefficients to determine specific heat capacity via Eq. A-64 [36]

$\bar{m}_{\text{alk}}$	1.8-10.9 m
range	
t	40-120 °C
α	0-0.583
$c_{\text{Cp},0}$	4.294E+00
$c_{\text{Cp},1}$	−1.859E−03
$c_{\text{Cp},2}$	2.575E−05
$c_{\text{Cp},3}$	−7.819E−01
$c_{\text{Cp},4}$	6.536E−01
$c_{\text{Cp},5}$	−1.124E−01
$c_{\text{Cp},6}$	4.746E−03
$c_{\text{Cp},7}$	8.181E−04
$c_{\text{Cp},8}$	8.267E−05
$c_{\text{Cp},9}$	−5.364E−02
$c_{\text{Cp},10}$	−1.909E−04
n^*	160
$\sigma^\dagger$	0.74 %

$^*n$ is the number of data points

$^\dagger\sigma = \frac{1}{n}\sum_1^n \left(\frac{|\rho_{\text{p,exp}} - \rho_{\text{p,calc}}|}{\rho_{\text{p,exp}}}\right)$

Table A-9: Coefficients to determine CO_2 solubility via Eq. A-65 [36]

$\bar{m}_{\text{alk}}$	7 m
M_{alk}	61.08 g/mol
range	
t	25-120 °C
α	0.03-0.58
$c_{\text{pco2},0}$	22.53
$c_{\text{pco2},1}$	-7904
$c_{\text{pco2},2}$	105.0
$c_{\text{pco2},3}$	-16810
$c_{\text{pco2},4}$	-286.4
$c_{\text{pco2},5}$	26480
$c_{\text{pco2},6}$	381.70
$c_{\text{pco2},7}$	8295
$c_{\text{pco2},8}$	-257.4
n^*	87
$\sigma^\dagger$	16.7 %

$^*n$ is the number of data points

$^\dagger\sigma = \frac{1}{n}\sum_1^n \left(\frac{|p^*_{\text{CO2,exp}} - p^*_{\text{CO2,calc}}|}{p^*_{\text{CO2,exp}}}\right)$

$$f_0 = \frac{\mathrm{C}_1}{Re} + \frac{\mathrm{C}_2}{Re^{1/2}} + \mathrm{C}_3 \tag{A-69}$$

Change in bed void fraction

$$\varepsilon^{'} = \varepsilon - \varepsilon^{\mathrm{liq}} \tag{A-70}$$

Change in particle diameter

$$d_{\mathrm{p}}^{'} = d_{\mathrm{p}} \left(\frac{1 - \varepsilon \ \left(1 - \varepsilon^{\mathrm{liq}}/\varepsilon\right)}{1 - \varepsilon} \right)^{1/3} \tag{A-71}$$

Where particle diameter is

$$d_{\mathrm{p}} = \frac{6(1-\varepsilon)}{a} \tag{A-72}$$

$$f_0^{'} = f_0 \left(\frac{-\varepsilon \left(1 - \varepsilon^{\mathrm{liq}}/\varepsilon\right)}{1 - \varepsilon} \right)^{\mathrm{c}/3} \tag{A-73}$$

Where c is calculated by

$$c = \frac{-\mathrm{C}_1/Re - \mathrm{C}_2/(2Re^{1/2})}{f_0} \tag{A-74}$$

Pressure drop per unit of length

$$\frac{\Delta p_{\mathrm{irr}}}{Z} = \frac{3}{4} f_0^{'} \left((1 - \varepsilon^{'})/\varepsilon^{'4.65} \right) \rho_{\mathrm{g}} U_{\mathrm{g}}^2 / d_{\mathrm{p}}^{'} \tag{A-75}$$

Model input and output variables and parameters

As the Packed Column model is a model with a R-S type module, the pressure at the outlet is the input variable for the model, and the The Stichlmair constants depend on the type of packing.

Table A-10: Model input and output variables and parameters for the pressure drop module

Input variables	$P_{\mathrm{n+1}}$, $\dot{V}_{\mathrm{in}}$, $\varepsilon_{\mathrm{n}}^{\mathrm{liq}}$, $\varepsilon_{\mathrm{dyn}}^{\mathrm{liq}}$
Output variables	$P_{\mathrm{in}}^{\mathrm{vap}}$, $\dot{V}_{\mathrm{n}}^{\mathrm{vap}}$, h
Parameters	C_1, C_2, C_3, ε, a

A-9 Stichlmair hold up correlation

Component description

Relevant phenomena

- Hold up of liquid in the packing

Hypothesis and assumptions

- The liquid is evenly distributed over the packing

Model equations

Total hold up

$$\varepsilon_{\mathrm{n}}^{\mathrm{liq}} = \varepsilon_{\mathrm{stat}}^{\mathrm{liq}} + \varepsilon_{\mathrm{dyn}}^{\mathrm{liq}} \tag{A-76}$$

Static hold up [38]

$$h_{\mathrm{stat}} = 0.033^{-0.22\ \frac{g\ \rho_{\mathrm{L}}}{\sigma_{\mathrm{L}}\ a^2}} \tag{A-77}$$

Dynamic hold up [39]

$$h_{\mathrm{dyn,0}} = 0.555\ Fr_{\mathrm{L}}^{1/3} \tag{A-78}$$

$$Fr_{\mathrm{L}} = U_{\mathrm{L}}^2\ \frac{a}{g\ \varepsilon^{4.65}} \tag{A-79}$$

$$h_{\mathrm{dyn}} = h_{\mathrm{dyn,0}} \left(1 + 20 \left(\frac{\Delta p_{\mathrm{irr}}}{Z \rho_{\mathrm{L}} g}\right)^2\right) \tag{A-80}$$

Model input and output variables and parameters

Table A-11: Model input and output variables for the hold up module

Input variables	$P_{\mathrm{n+1}}^{\mathrm{vap}}$, $\varepsilon_{\mathrm{n}}^{\mathrm{liq}}$
Output variables	$\varepsilon_{\mathrm{stat}}^{\mathrm{liq}}$, $\dot{V}_{\mathrm{n}}^{\mathrm{liq}}$, $\varepsilon_{\mathrm{dyn}}^{\mathrm{liq}}$
Parameters	ε, a

A-10 Controller settings

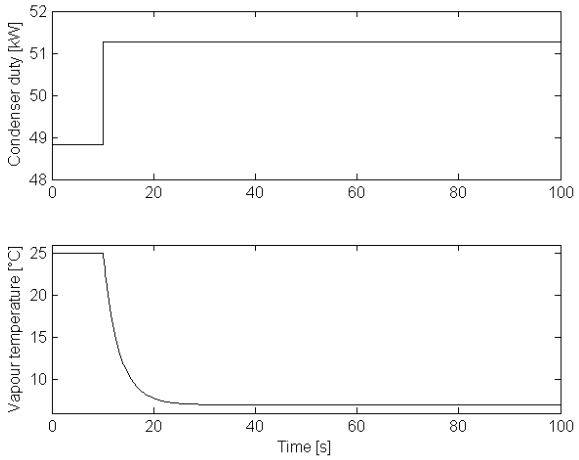

Figure A-7: Condenser open-loop step response

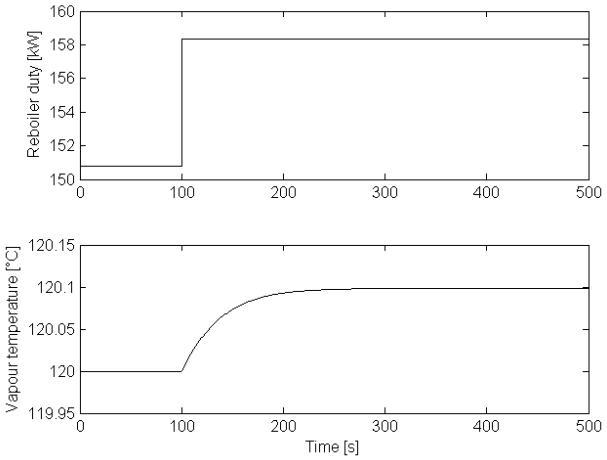

Figure A-8: Reboiler open-loop step response

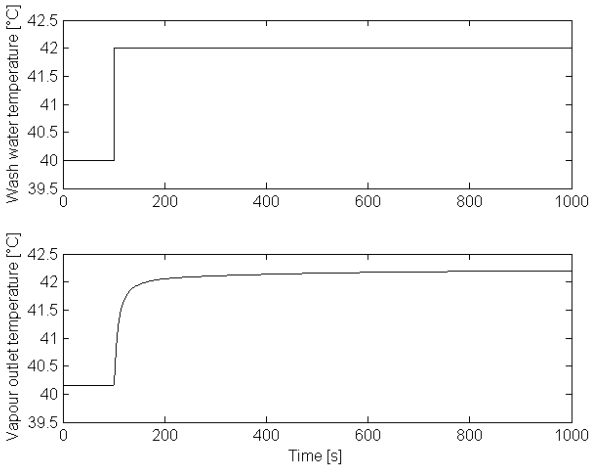

Figure A-9: Washing section open-loop step response

Appendix B

Results

This appendix contains additional data and results for Chapters 4 and 5.

B-1 Measurement methods

B-1-1 Density

The density of the solvent has been measured with the density measurement device Anton Paar DMA 4500. The density is measured in duplicate to decrease the measurement error. Before every measurement the device is rinsed with the solvent and after every measurement the device is rinsed with water. The average of the two measurements is used for further calculations.

Figure B-1: The used device for the measurement of the solvent density

B-1-2 Solvent concentration

To determine the monoethanolamine (MEA) concentration, the solvent has been titrated with a Titralab TIM965 titrator. As the MEA is a base, a solution of 0.1M HCl has been used as a titrant. Of the solvent 100μL was pipetted and topped up with demineralized water. Then, the titrant is added to the analyte at a speed of 1 mL/min until the inflection point has passed. With the amount of titrant added at the inflection point the unknown MEA molarity can be calculated. This measurement has also been performed in duplicate to reduce the measurement error.

B-1-3 Solvent loading

To determine the solvent loading, measurement of the CO_2 concentration is required. As the CO_2 is bound to the MEA in the solvent, it is difficult to measure it. To measure the CO_2 concentration a phosphoric acid set-up has been used. In this set-up a sample of 5 mL of solvent is injected in boiling phosphoric acid to release the CO_2. A circulation gas discharges the CO_2 and cools it in a cold trap to knock out water vapor. The gas is then analysed in a CO_2 analyser and the CO_2 concentration is monitored in time. By integrating the CO_2 gas concentration in time the total amount of CO_2 in the sample can be determined.

Figure B-2: The phosphoric acid setup for the measurement of the solvent CO_2 loading

B-2 Solvent data

Table B-1: Solvent measurements and calculated solvent concentration and loadings for test A1 (flue gas step decrease)

Time [min]	Sample place	MEA [mol/L]	CO_2 [mol/L]	Density [kg/m^3]	MEA wt% [kg/kg]	loading [mol/mol]
−10	rich	5.017	2.421	1.1123	29.8	0.483
−10	lean	5.218	1.229	1.0687	32.3	0.236
0	rich		2.374			0.473
0	lean		1.222			0.236
10	rich		2.387			0.476
10	lean		1.310			0.251
20	rich		2.277			0.454
20	lean		1.231			0.236
30	rich		2.256			0.450
30	lean		1.215			0.233
60	rich		2.188			0.436
60	lean		1.216			0.233
120	rich		2.211			0.437
120	lean		2.168			0.229

Table B-2: Solvent measurements and calculated solvent concentration and loadings for test A2 (flue gas step decrease)

Time [min]	Sample place	MEA [mol/L]	CO_2 [mol/L]	Density [kg/m^3]	MEA wt% [kg/kg]	loading [mol/mol]
−10	rich	5.057	2.211	1.1045	30.3	0.437
−10	lean	5.246	1.197	1.0668	32.5	0.228
0	rich		2.168			0.429
0	lean[1]		-			-
10	rich		2.254			0.446
10	lean		1.204			0.230
26	rich		2.389			0.473
26	lean		1.194			0.228
30	rich		2.363			0.467
30	lean		1.209			0.231
60	rich		2.390			0.473
60	lean		1.196			0.228
120	rich		2.466			0.488
120	lean		1.248			0.238

[1]This sample is missing

Table B-3: Solvent measurements and calculated solvent concentration and loadings for test B1 (solvent step increase)

Time [min]	Sample place	MEA [mol/L]	CO_2 [mol/L]	Density [kg/m^3]	MEA wt% [kg/kg]	loading [mol/mol]
−10	rich	5.017	2.466	1.1131	29.8	0.492
−10	lean	5.157	1.248	1.0682	31.9	0.242
0	rich		2.406			0.480
0	lean		1.269			0.246
10	rich		2.325			0.463
10	lean		1.455			0.282
20	rich		2.219			0.442
20	lean		1.306			0.253
30	rich		2.231			0.445
30	lean		1.307			0.254

B-3 Parameter fitting

Table B-4: Model results for variation of the heat transfer coefficient in the rich/lean heat exchanger for a lean solvent flow rate of 3.2 ton/h, rich solvent flow rate of 3.09 m^3/h, rich inlet temperature of 51.38 °C and a lean inlet temperature of 120.31 °C. The best fit according to the rich outlet temperature is highlighted in bold.

Heat transfer coefficient [W/m^2K]	Rich outlet temperature [°C]	Lean outlet temperature [°C]
1000	107.48	64.08
1100	108.38	63.04
1200	109.15	62.14
1300	109.81	61.36
1400	**110.40**	**60.68**
1500	110.91	60.08
1600	111.37	59.54
1700	111.77	59.06
1800	112.14	58.62
1900	112.47	58.23
2000	112.77	57.87
pilot	**110.46**	**59.58**

Table B-5: Model results for variation of the heat transfer coefficient in the lean solvent cooler for a lean solvent flow rate of 3.2 ton/h, solvent inlet temperature of 59.58 °C and a cooling water inlet temperature of 19.06 °C. The cooling water flow controller is set to 40 °C. The best fit according to the cooling water flow is highlighted in bold.

Heat transfer coefficient [W/m^2K]	Cooling water outlet temperature [°C]	Cooling water flow [m^3/h]
1000	53.48	1.53
1100	54.81	1.47
1200	55.82	1.43
1300	56.59	1.40
1400	57.18	1.38
1500	**57.65**	**1.36**
1600	58.02	1.35
1700	58.31	1.34
1800	58.54	1.33
1900	58.73	1.33
2000	58.89	1.32
pilot	**57.20**	**1.36**

B-4 Temperature profiles

On the following pages the absorber temperature profiles of both the model and the experiments at the pilot capture plant for the tests A1,A2 and B1 are shown.

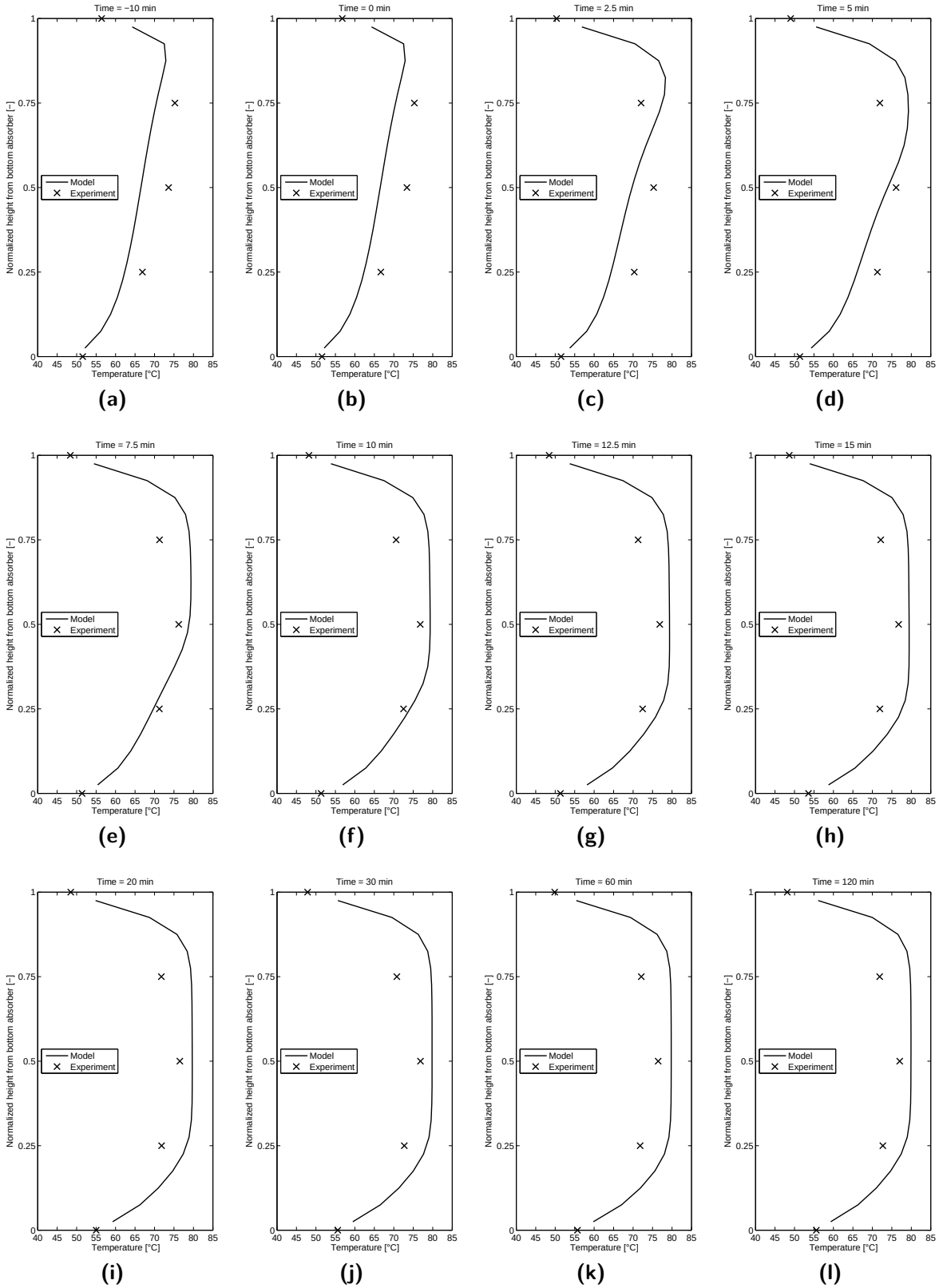

Figure B-3: Comparison of the absorber temperature profiles in time of the model and the experiment for test A1 (flue gas step increase)

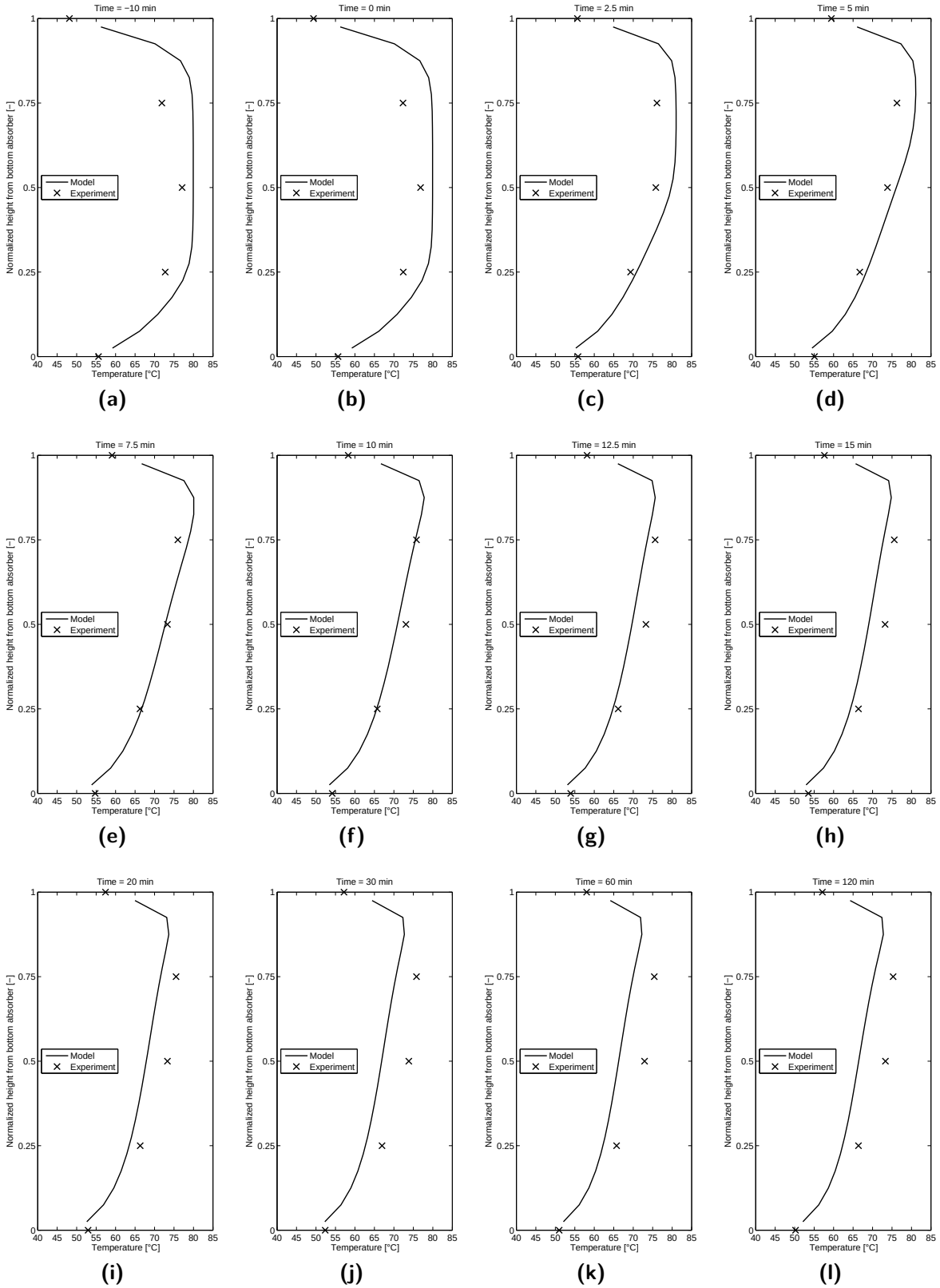

Figure B-4: Comparison of the absorber temperature profiles in time of the model and the experiment for test A2 (flue gas step decrease)

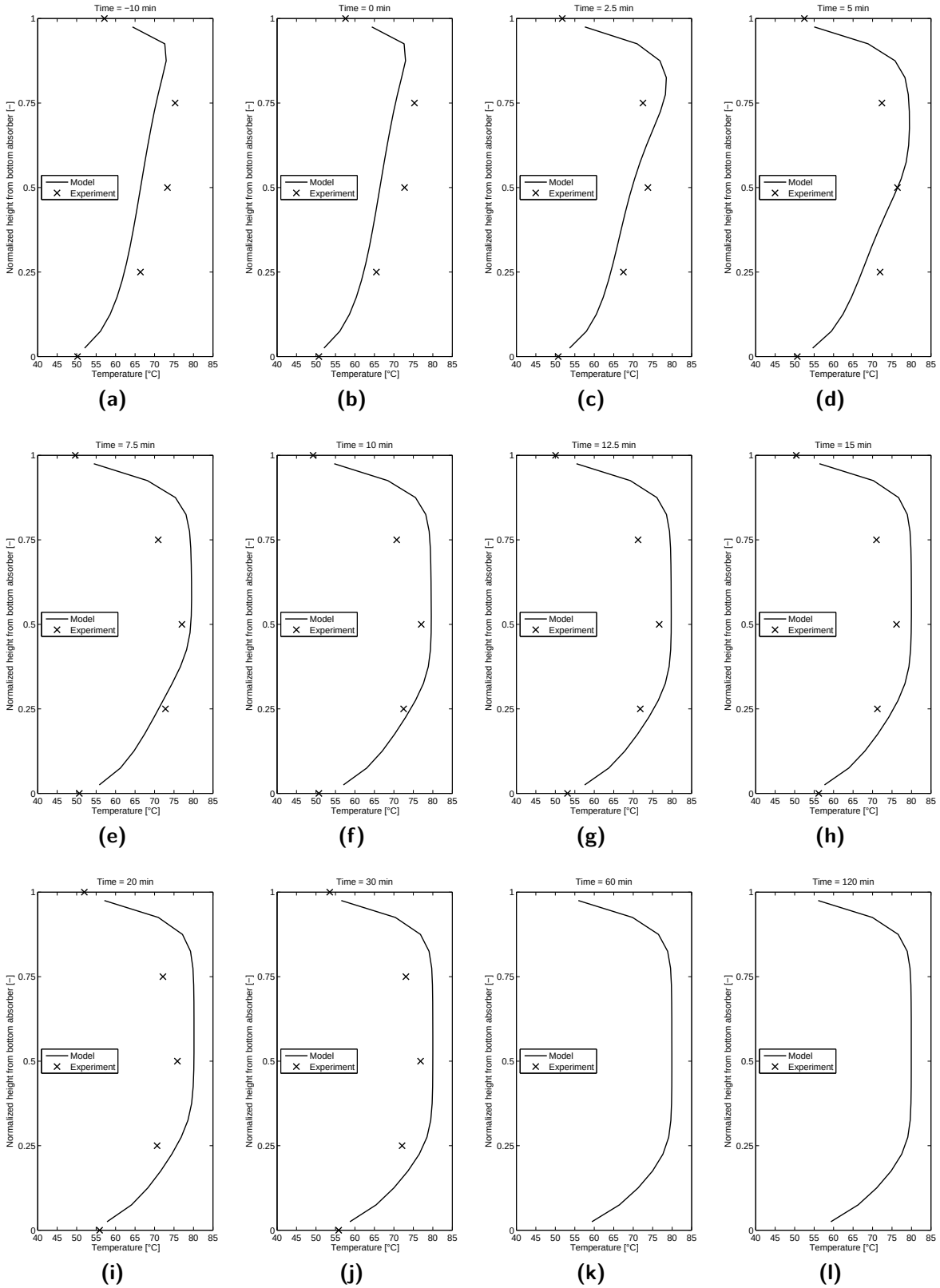

Figure B-5: Comparison of the absorber temperature profiles in time of the model and the experiment for test B1 (solvent step increase)

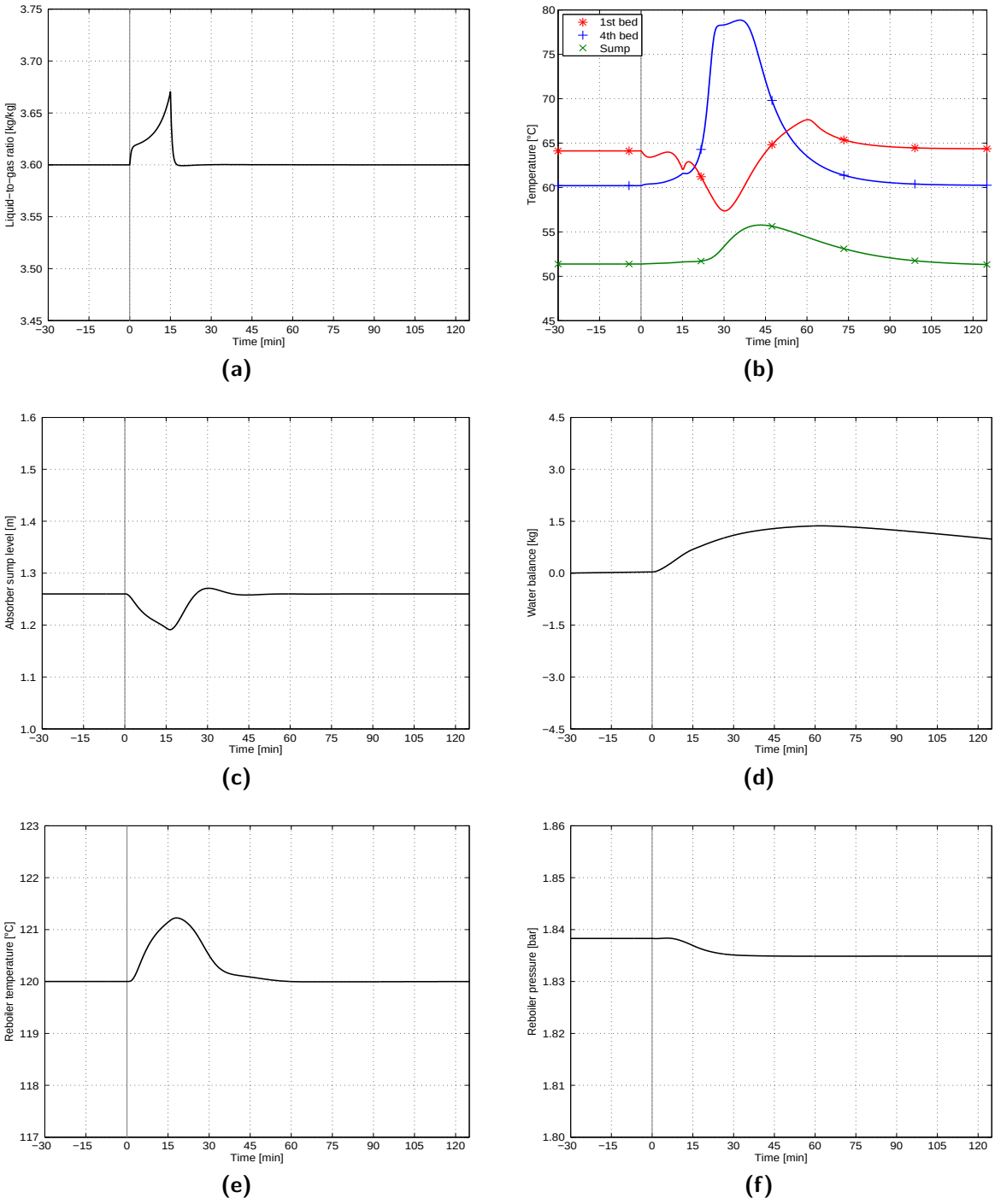

Figure B-6: System response to a decrease of the flue gas flow rate (Case A) of the liquid-to-gas ratio ratio (a), absorber temperatures (b), absorber sump level (c), system water balance (d), reboiler temperature (e) and reboiler pressure (f)

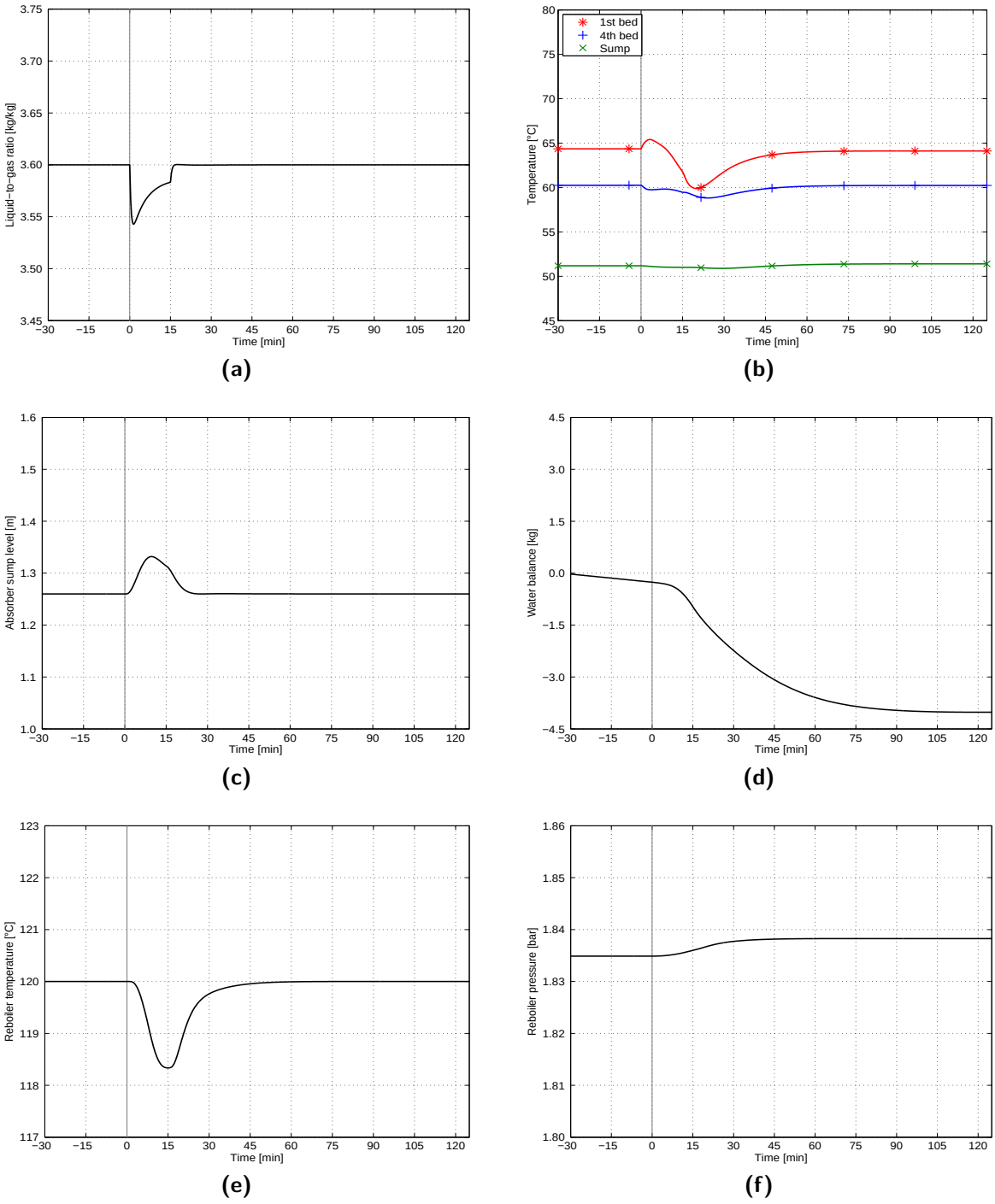

Figure B-7: System response to a increase of the flue gas flow rate (Case B) of the liquid-to-gas ratio ratio (a), absorber temperatures (b), absorber sump level (c), system water balance (d), reboiler temperature (e) and reboiler pressure (f)

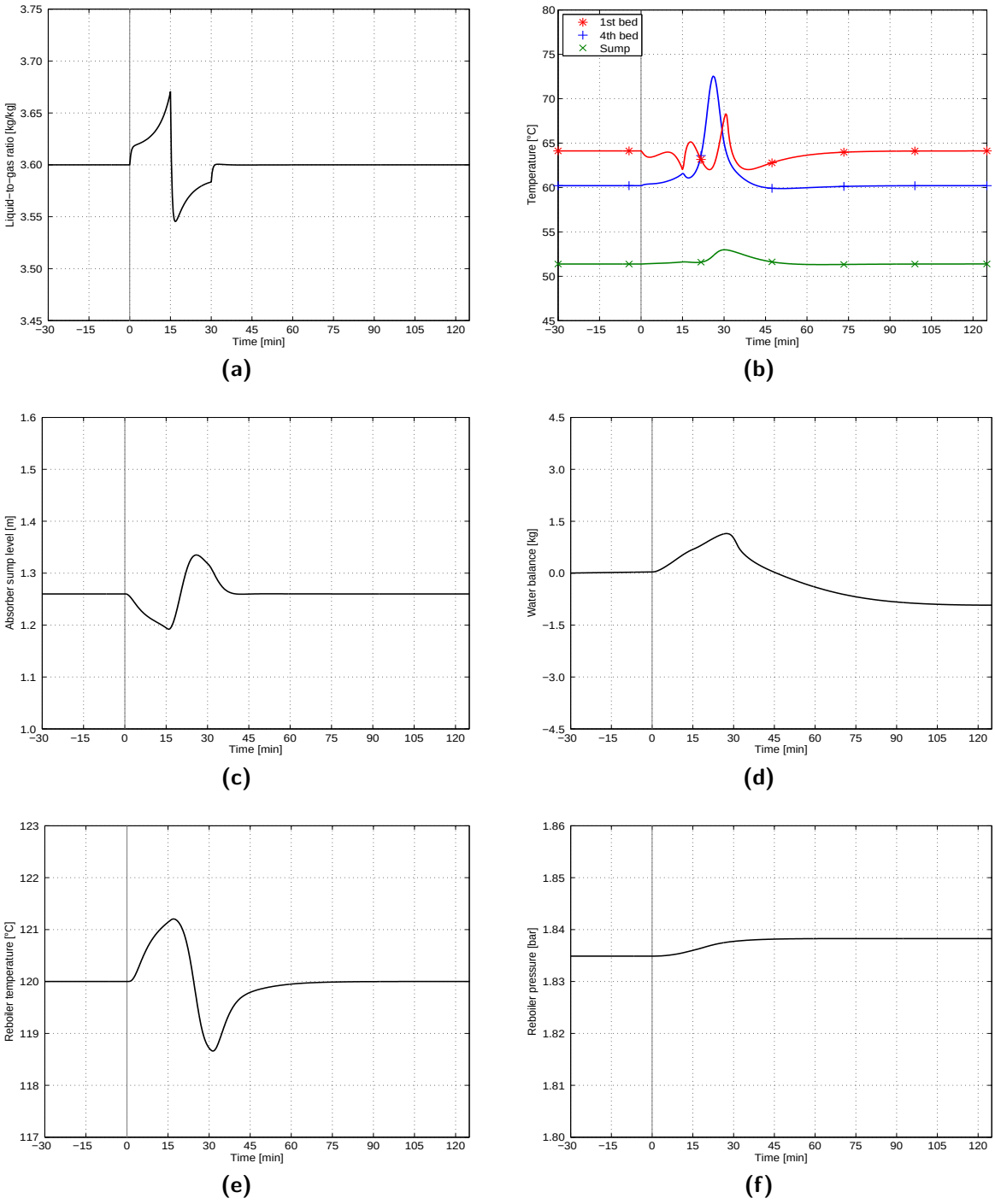

Figure B-8: System response to a decrease followed by an immediate increase of the flue gas flow rate (Case C) of the liquid-to-gas ratio ratio (a), absorber temperatures (b), absorber sump level (c), system water balance (d), reboiler temperature (e) and reboiler pressure (f)

Bibliography

[1] IEA (International Energy Agency), "CO_2 emissions from fuel combustion," tech. rep., OECD/IEA, France, 2012.

[2] B. Metz, O. Davidson, H. de Coninck, M. Loos, and L. Meyer, "IPCC special report on carbon dioxide capture and storage," tech. rep., IPCC, 2005.

[3] Technology Roadmap: Carbon capture and storage tech. rep., International Energy Agency, 2009.

[4] Global CCS institute, "The global status of CCS:2011," tech. rep., 2011.

[5] IEA (International Energy Agency), "Energy technology perspective," tech. rep., OECD/IEA, France, 2012.

[6] EPRI (Electric Power Research Institute), "CO_2 capture technologies," tech. rep., 2011.

[7] CO2 CRC, The Cooperative Research Centre for Greenhouse Gas Technologies , URL: http://www.co2crc.com.au/imagelibrary3/capture.php.

[8] I. Pfaff, J. Oexmann, and A. Kather, "Optimised integration of post-combustion CO_2 capture process in greenfield power plants," *Energy*, vol. 35, no. 10, pp. 4030–4041, 2010.

[9] H. Moe, *Dynamic Process Simulation: Studies on Modeling and Index Reduction.* Doktor ingeniøravhandling, University of Trondheim, Norwegian Institute of Technology, Department of Chemical Engineering, 1995.

[10] R. Gani and I. T. Cameron, "Modelling for dynamic simulation of chemical processes: the index problem," *Chemical engineering science*, vol. 47, no. 5, pp. 1311–1315, 1992.

[11] L. F. Shampine, M. W. Reichelt, and J. A. Kierzenka, "Solving index-1 DAEs in MATLAB and simulink," *SIAM review*, vol. 41, no. 3, pp. 538–552, 1999.

[12] J. D. Pryce, "A simple structural analysis method for DAEs," *BIT Numerical Mathematics*, vol. 41, no. 2, pp. 364–394, 2001.

[13] P. Moin, *Fundamentals of engineering numerical analysis.* Cambridge University Press, 2010.

[14] F. E. Cellier, H. Elmqvist, and M. Otter, "Modeling from physical principles," in *The Control Handbook*, Citeseer, 1996.

[15] N. Hogan and P. C. Breedveld, "The physical basis of analogies in network models of physical system dynamics," in *International Conference on Bond Graph Modeling and Simulation*, 1999.

[16] F. Casella, J. van Putten, and P. Colonna, "Dynamic simulation of a biomass-fired steam power plant: a comparison between causal and a-causal modular modeling," ASME, 2007.

[17] I. T. Cameron and K. Hangos, *Process modelling and model analysis*, vol. 4. Academic Press, 2001.

[18] P. Colonna and H. Van Putten, "Dynamic modeling of steam power cycles.: Part i - modeling paradigm and validation," *Applied Thermal Engineering*, vol. 27, no. 2, pp. 467–480, 2007.

[19] H. van Putten, *Integrated modelling for improving the design and operation of steam power plants*. PhD thesis, TU Delft, 2008.

[20] H. M. Kvamsdal, J. Jakobsen, and K. Hoff, "Dynamic modeling and simulation of a CO_2 absorber column for post-combustion CO_2 capture," *Chemical Engineering and Processing*, vol. 48, pp. 135–144, 2009.

[21] K. Dietl, A. Joos, and G. Schmitz, "Dynamic analysis of the absorption-desorption loop of a carbon capture plant using an object oriented approach," *Chemical Engineering and Processing*, vol. 52, pp. 132–139, 2012.

[22] A. Joos, K. Dietl, and G. Schmitz, "Thermal Separation: An approach for a Modelica library for absorption, adsorption and rectification," in *Linköping Electronic Conference Proceedings* (F. Casella, ed.), pp. 804–813, Linköping University Electronic Press, september 2009.

[23] A. Lawal, M. Wang, and P. Stephenson, "Demonstrating full-scale post-combustion CO_2 capture for coal-fired power plants through dynamic modeling and simulation," *Fuel*, 2010.

[24] J. Akesson, R. Faber, C. Laird, K. Prölß, H. Tummesheit, S. Velut, and Y. Zhu, "Models of a post-combustion absorption unit for simulation, optimization and non-linear model predictive control schemes," Modelica Association, 2011.

[25] R. Faber, M. Köpcke, O. Biede, J. N. Knudsen, and J. Andersen, "Open-loop step responses for the MEA post-combustion capture process: Experimental results from the Esjberg pilot plant," *Energy Procedia*, vol. 4, pp. 1427–1434, 2011.

[26] The Modelica Association , Modelica home page, URL: http://www.modelica.org/.

[27] F. Casella and A. Leva, "Modelling of thermo-hydraulic power generation processes using Modelica," *Mathematical and Computer Modelling of Dynamical Systems*, vol. 1, pp. 19–33, 2006.

[28] Dymola, Dynamic Modeling Library , URL: http://www.dymola.com/.

[29] CATO-2 program website , URL: http://www.co2-cato.nl/.

[30] Aspen Technology, Inc., Aspen Plus Software V7.3 , URL: http://www.aspentech.com.

[31] Aspen Technology, Inc., *ASPEN PLUS User Guide version 10.2*. 2000.

[32] P. Colonna, "Modeling and simulation of energy conversion systems (WB4431-05)." lecture notes, TU Delft, 2010.

[33] I.-L. Chien, "Consider IMC tuning to improve controller performance," *Chemical Engineering Progress*, vol. 86, pp. 33–41, 1990.

[34] D. E. Seborg, D. A. Mellichamp, T. F. Edgar, and F. J. Doyle III, *Process dynamics and control*. Wiley, 2010.

[35] S. Skogestad, "Simple analytic rules for model reduction and PID controller tuning," *Journal of process control*, vol. 13, no. 4, pp. 291–309, 2003.

[36] J. Oexmann, *Post-combustion CO_2 capture: energetic evaluation of absorption processes in coal-fired steam power plants*. PhD thesis, Technischen Universität Hamburg-Harburg, 2011.

[37] J. Stichlmair, J. Bravo, and J. Fair, "General model for prediction of pressure drop and capacity of countercurrent gas/liquid packed columns," *Gas Separation & Purification*, vol. 3, no. 1, pp. 19–28, 1989.

[38] V. Engel, "Fluiddynamik in füllkörper-undpackungskolonnen für gas/flüssig-systeme," *Chemie Ingenieur Technik*, vol. 72, no. 7, pp. 700–703, 2000.

[39] I. Wagner, J. Stichlmair, and R. James, "Mass transfer in beds of modern, high-efficiency random packings," *Industrial & engineering chemistry research*, vol. 36, no. 1, pp. 227–237, 1997.

Glossary

List of Acronyms

MEA	monoethanolamine
GHG	greenhouse gases
CCS	carbon capture and storage
IEA	International Energy Agency
PCC	Post-combustion capture
BDU	Brownian Demister Unit
FGD	flue gas desulphurization
RES	renewable energy sources
IGCC	Integrated Gasification Combined Cycle
PFD	Process Flow Diagram
DAEs	differential and algebraic equations
ODEs	ordinary differential equations
CCU	carbon capture unit
P&ID	process and instrumentation diagram

List of symbols

Symbols:

A	[m^2]	Area
a	[m^2/m^3]	Specific area
C	[J/kg]	Specific heat capacity
c	[mol/m^3]	Molar concentration
dp	[m]	Particle diameter
F	[N]	Force
Fr	[-]	Froude number
G	[kg.m/s]	Total momentum
g	[m/s^2]	Gravitational acceleration
H	[m]	Height of the packing
M	[kg]	Total mass
MM	[kg/mol]	Molar mass
$\dot{\mathbf{m}}$	[kg/s]	Mass flow rate
$\bar{\mathbf{m}}$	[mol/kg]	Molarity
N	[mol]	Total moles
$\dot{\mathbf{N}}$	[mol/s]	Molar flow rate
P	[Pa]	Pressure
$\mathbf{p}^*$	[Pa]	Partial pressure
Q	[J]	Heat added to the system
R	[J/(mol.K)]	Ideal gas constant
Re	[-]	Reynolds number
S	[m^2]	Surface
T	[K]	Temperature
t	[°C]	Temperature
U	[J]	Total internal energy
V	[m^3]	Volume
$\dot{\mathbf{V}}$	[m^3/s]	Volumetric flow rate
v	[m/s]	Velocity
$\dot{\mathbf{W}}$	[J]	Work done by the system
x	[mol/mol]	Liquid molar composition

Greek letters:

$\boldsymbol{\alpha}$	[mol/mol]	Loading
$\boldsymbol{\varepsilon}$	[m^3/m^3]	Void fraction
$\boldsymbol{\mu}$	[Pa.s]	Dynamic viscosity
$\boldsymbol{\rho}$	[kg/m^3]	Density
$\boldsymbol{\Omega}$	[m]	Perimeter

Subscripts/superscripts:

alk	Alkali
dyn	Dynamic
ff	Friction force
E	Entering
fric	Frictional
g	Gas
i	Component i
in	Inlet
j	Stage j
L	Leaving
liq	Liquid
n	On the n^{th} stage
nom	Nominal
out	Outlet
p	Particle
S	Shaft
stat	Static
vap	Vapour